The Abdus Salam
International Centre for Theoretical Physics

United Nations
Educational, Scientific and
Cultural Organization

IAEA
International Atomic Energy Agency

2165-17

International MedCLIVAR-ICTP-ENEA Summer School on the Mediterranean Climate System and Regional Climate Change

13 - 22 September 2010

Land-Atm Interaction: land surface and extreme climate events: observations and an idealized model

D'ANDREA Fabio
LMD-ENS
Paris
France

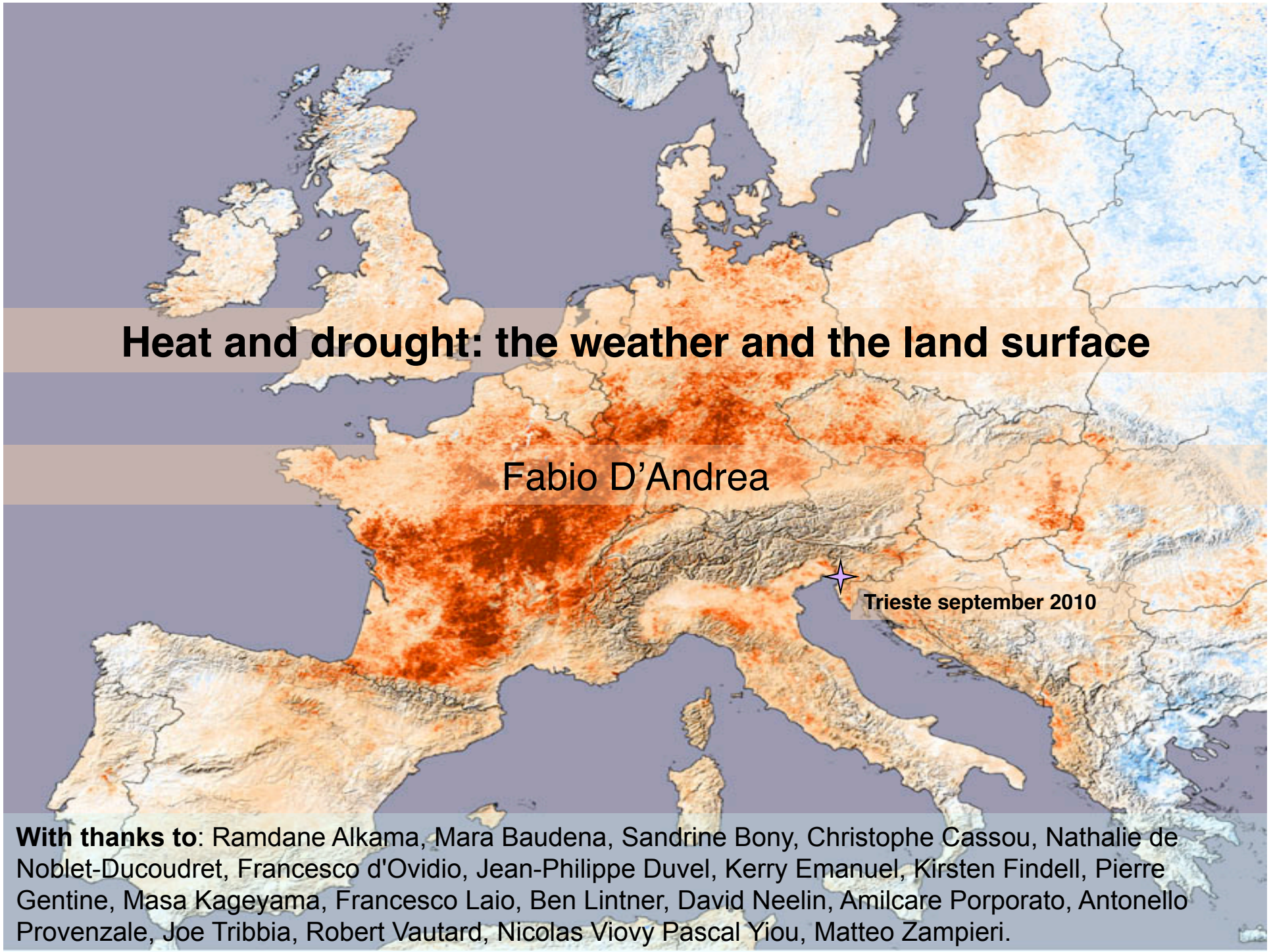

Heat and drought: the weather and the land surface

Fabio D'Andrea

With thanks to: Ramdane Alkama, Mara Baudena, Sandrine Bony, Christophe Cassou, Nathalie de Noblet-Ducoudret, Francesco d'Ovidio, Jean-Philippe Duvel, Kerry Emanuel, Kirsten Findell, Pierre Gentine, Masa Kageyama, Francesco Laio, Ben Lintner, David Neelin, Amilcare Porporato, Antonello Provenzale, Joe Tribbia, Robert Vautard, Nicolas Viovy Pascal Yiou, Matteo Zampieri.

Outline

1. Motivation

1.1 Climatology of a heatwave. Summer 2003.
1.2 Impacts, climate change.

2. The weather and the land surface

2.1 Synoptic aspects, internal dynamics and external forcing.
2.2 The importance of soil moisture and vegetation. Feedbacks.
2.3 “Hot spots” of land surface-climate coupling

3. An idealized study

3.1 A simple model of soil moisture - pbl interaction.
3.2 Feedbacks and multiple states
3.3 Effect of vegetation dynamics

3. Other mechanisms of soil moisture bimodality

3.1 Stochastic precipitation – Multiplicative noise
3.2 Soil processes – capillary rise of water
3.3 It’s not true – just an artifact of the seasonal cycle

1. Motivation

An extreme event : the 2003 heatwave in Europe

(Schär et al 2004, *Nature*)

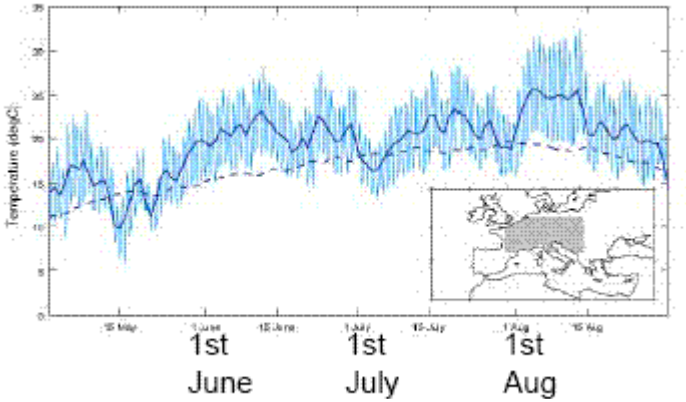

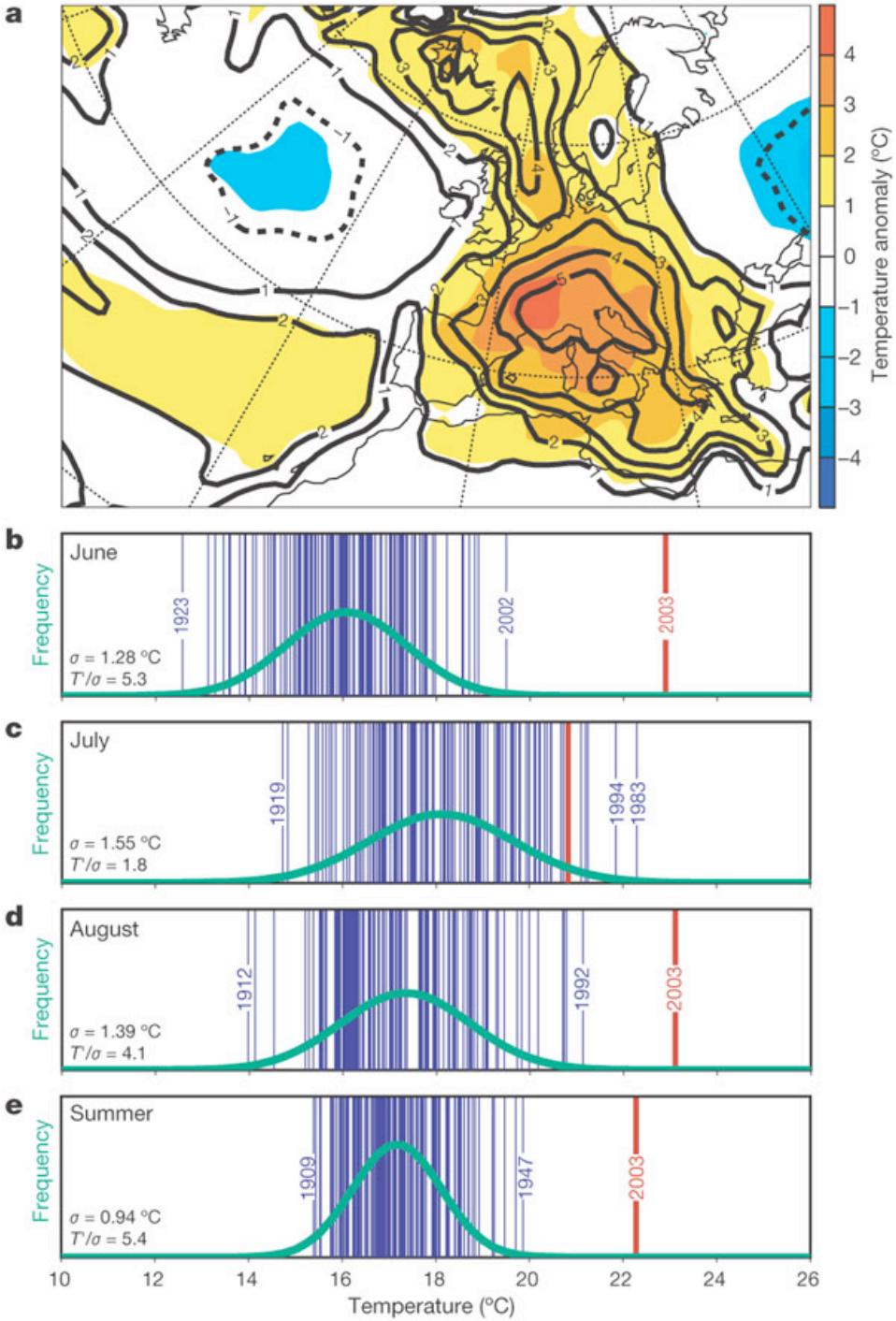

a, JJA temperature anomaly with respect to the 1961−90 mean. Colour shading shows temperature anomaly (°C), bold contours display anomalies normalized by the 30-yr standard deviation. **b−e**, Distribution of Swiss monthly and seasonal summer temperatures for 1864−2003. The fitted gaussian distribution is indicated in green. The values in the lower left corner of each panel list the standard deviation and the 2003 anomaly normalized by the 1864−2000 standard deviation (*T*'/*sigma).*

Increased mortality

http://ec.europa.eu/healt/ph_information/dissemination/unexpected/unexpected_1_en.htm

© European Communities, 1995-2006

FIGURE 1

Maximum central England temperature and daily mortality, England and Wales, July and August 2003

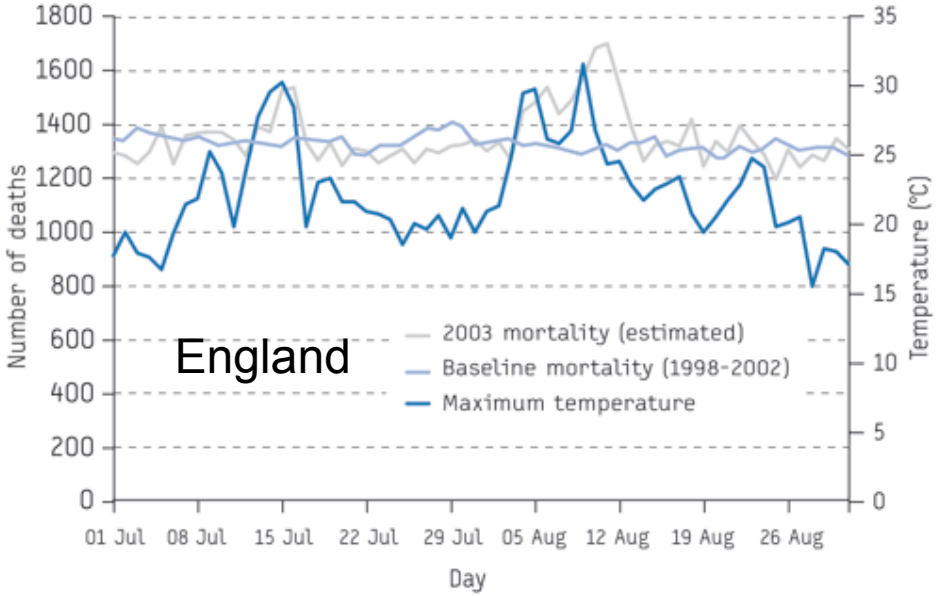

FIGURE

Daily excess of deaths during August 2003 and minimal and maximal daily temperatures, France

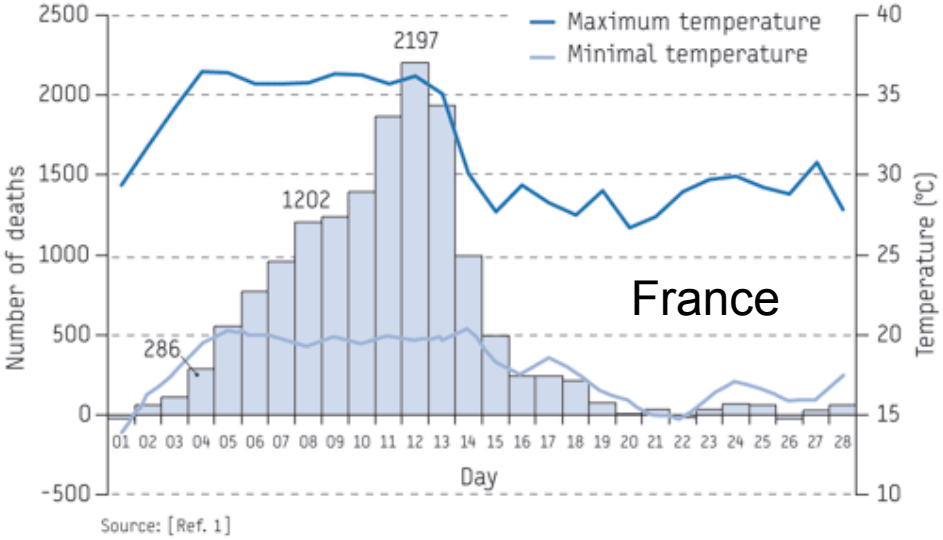

Source: [Ref. 1]

Mortality and average maximum temperature per week, The Netherlands, June-September 2003

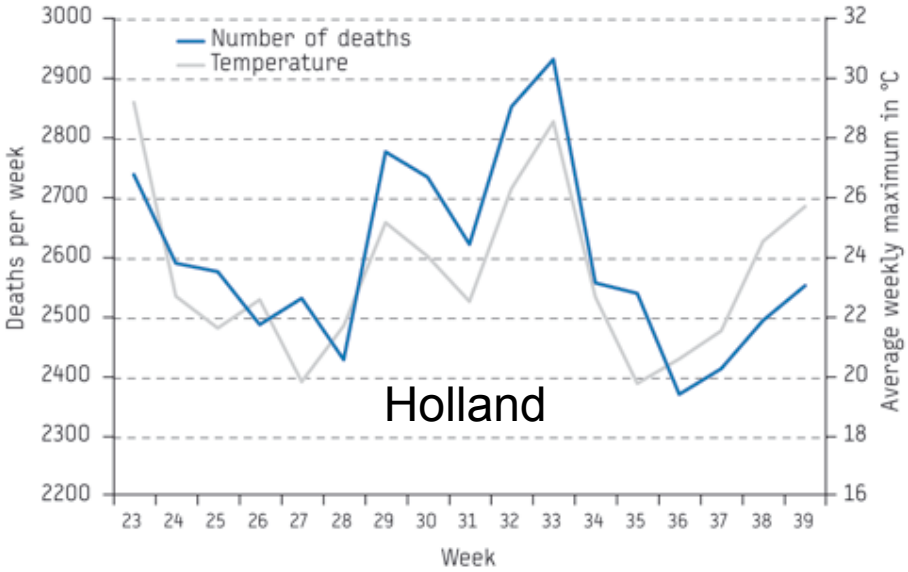

Forest fires in Portugal
August 3 2003.

Summer 2003 was the worst
in 23 years for forest fires.
5.6% of forest area was lost.

Decrease of agricultural production

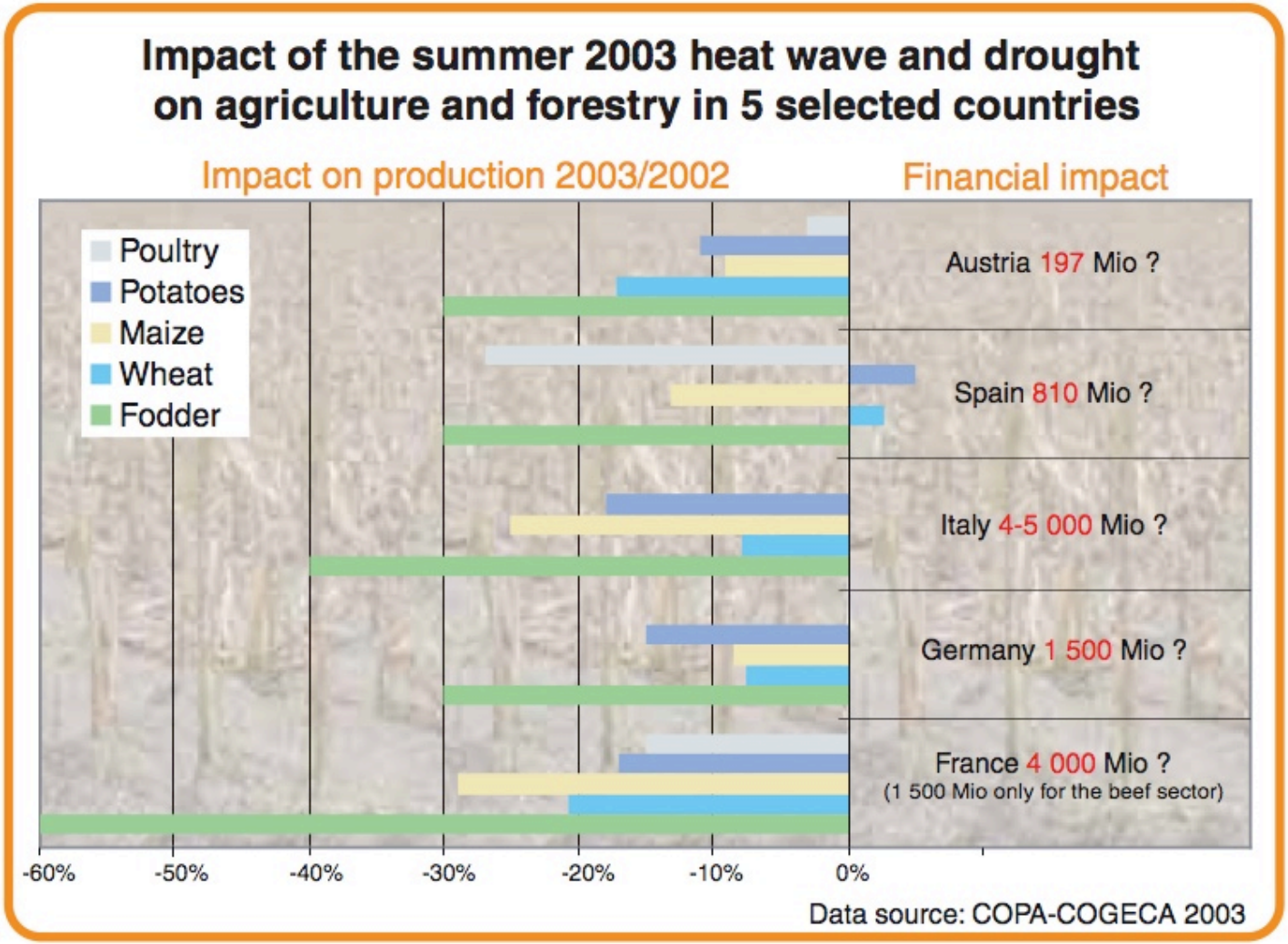

French fries

AGROJOB•NEWS

Rechercher une actualité mc RECHERCHE

BOURSE | ECONOMIE | ENTREPRISES | ENSEIGNES | FILIERES | FINANC

mc cain impact de la canicule sur les frites

Annonces Google Impact Testers Impact Systems Impact Barrier Impact Sockets

MC CAIN, impact de la canicule sur les frites

La canicule de ce début d'été a affecté différentes cultures : certains rendements comme le colza sont revus à la baisse de plus de 19%. Les cultures de pommes de terre dont la phase de croissance est tombée en pleine canicule (du 15 juillet au 15 août) ont, elles aussi, souffert. Et les pertes de rendements en qualité et quantité se font ressentir dans les industries agroalimentaires. Ainsi, le leader mondial des frites surgelées, MC CAIN, envisage une augmentation du prix de ses frites de 20 à 25% à partir du mois d'octobre.
A lui seul, le groupe MC CAIN consomme un million de pommes de terre par an (soit un quart de la production française) en provenance des régions Nord-Pas-de-Calais, Picardie et Champagne-Ardenne.
En France, le groupe emploie plus de 1 000 salariés sur 4 usines qui produisent 450 000 tonnes de frites.

- BASF et MOSANTO concluent un partenariat - [Le 22/03/2007]
- SUCRE, Sudzucker en difficulté - [Le 22/03/2007]
- COCA-COLA attaqué par la Bolivie - [Le 21/03/2007]

...

- Archives
- Agroalimentaire.fr

«L'hyperthermie est contreproductive pour l'activité sexuelle»

Par Charlotte Houang
LIBERATION.FR : Mercredi 26 juillet 2006 - 13:27

La canicule a t-elle des effets sur la sexualité ? Le docteur, Jacques Waynberg, sexologue et enseignant à Paris VIII , répond à Liberation.fr

La chaleur a t-elle des répercussions sur l'activité sexuelle ?

Une répercussion indirecte, très mal étudiée d'ailleurs. L'émotion érotique met en route des mécanismes : une augmentation du pouls, de la respiration et donc du stress. Faire l'amour est stressant et je ne voudrais pas fustiger les impuissants… Au-delà d'une certaine température, 30 à 35°, le corps est en surchauffe et donc aussi en stress. L'homme cherche par tous les moyens à faire baisser la température, si on ajoute à ça l'excitation érogène, il y a concurrence ! La chaleur est donc dissuasive puisque le corps féminin comme masculin est déjà stressé.

Mais ne dit-on pas que la sueur secrète des hormones ?

Le corps secrète plus d'hormones lorsqu'il est stressé, c'est vrai. Mais la température met le corps à l'épreuve, le coût énergétique le fatigue et tout devient plus éreintant. L'odeur de la sueur peut attirer lorsqu'il fait froid mais pas lorsque le corps est en surchauffe. D'ailleurs la performance sexuelle est diminuée par une trop forte chaleur. À moins d'être bien installé avec ventilateur et bougies parfumé, l'hyperthermie est contreproductive.

Donc les jeunes filles en tenue légère n'ont aucun effet sur les hommes ?

Les filles dénudées ne sont séduisantes et attirantes pour les hommes que dans un magasin climatisé ou chez Picard !

http://www.liberation.fr/actualite/societe/195532.FR.php

© Libération

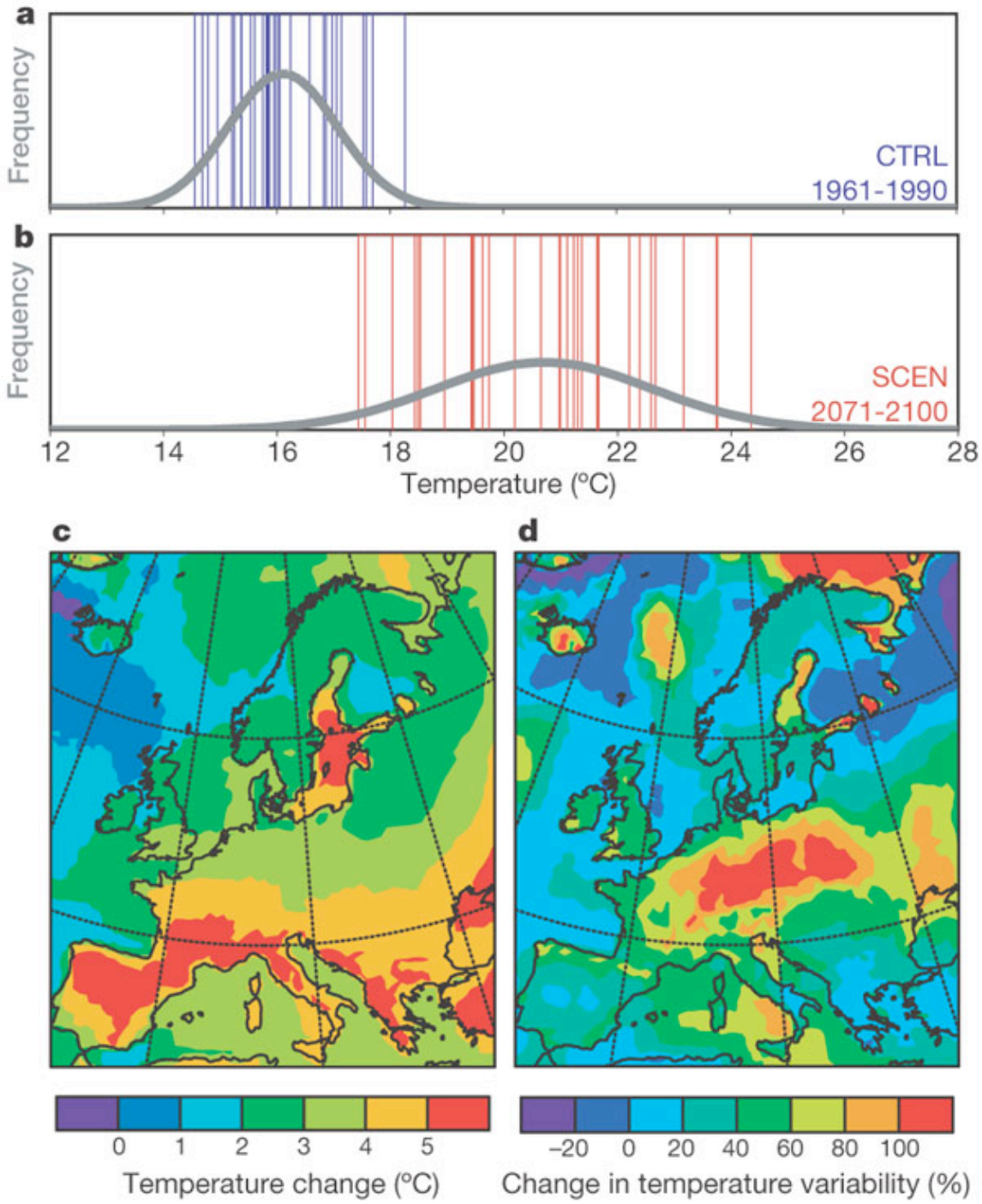

Climate Change
Variability change

a, b, Statistical distribution of summer temperatures at a grid point in northern Switzerland for CTRL and SCEN, respectively. c, Associated temperature change (SCEN\u2212CTRL, °C). d, Change in variability expressed as relative change in standard deviation of JJA means ((SCEN\u2212CTRL)/CTRL, %).

Schär et al 2004 *Nature*

2. The weather and the land surface

Synoptic aspect 2003

(Black and Sutton 2004)

Prevailing anticyclonic conditions.

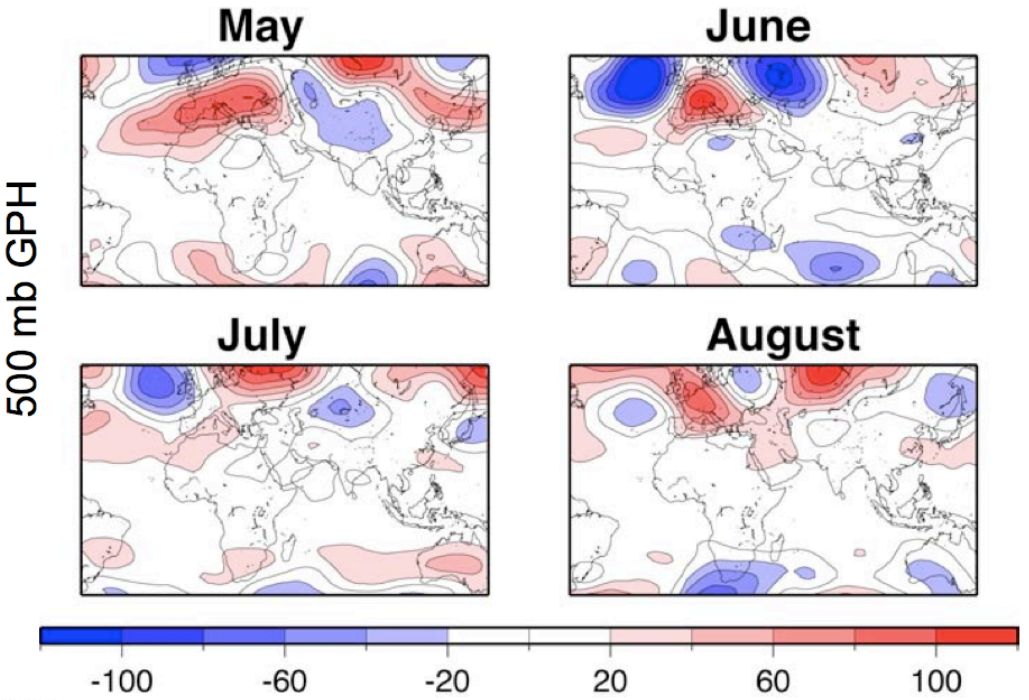

Anomalous SST

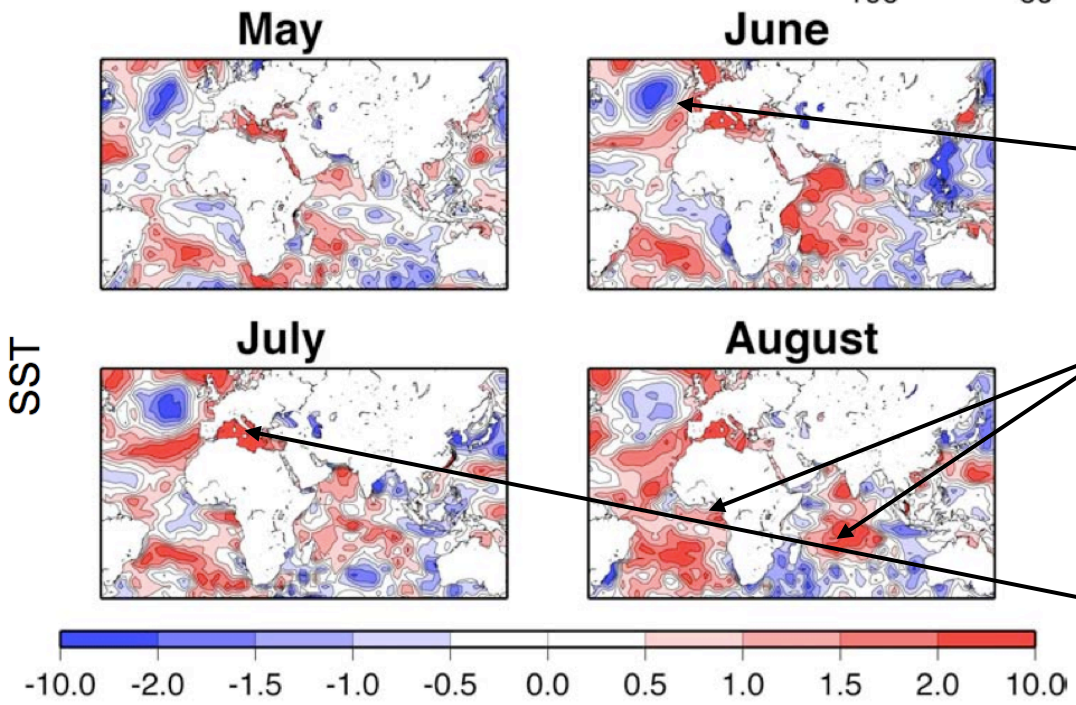

"Horseshoe" pattern

Hot Indian and tropical Atlantic ocean

Hot Mediterranean

Summer Weather Regimes
And their associated Temperature anomalies.

(Cassou et al 2005, *J. Clim*.)

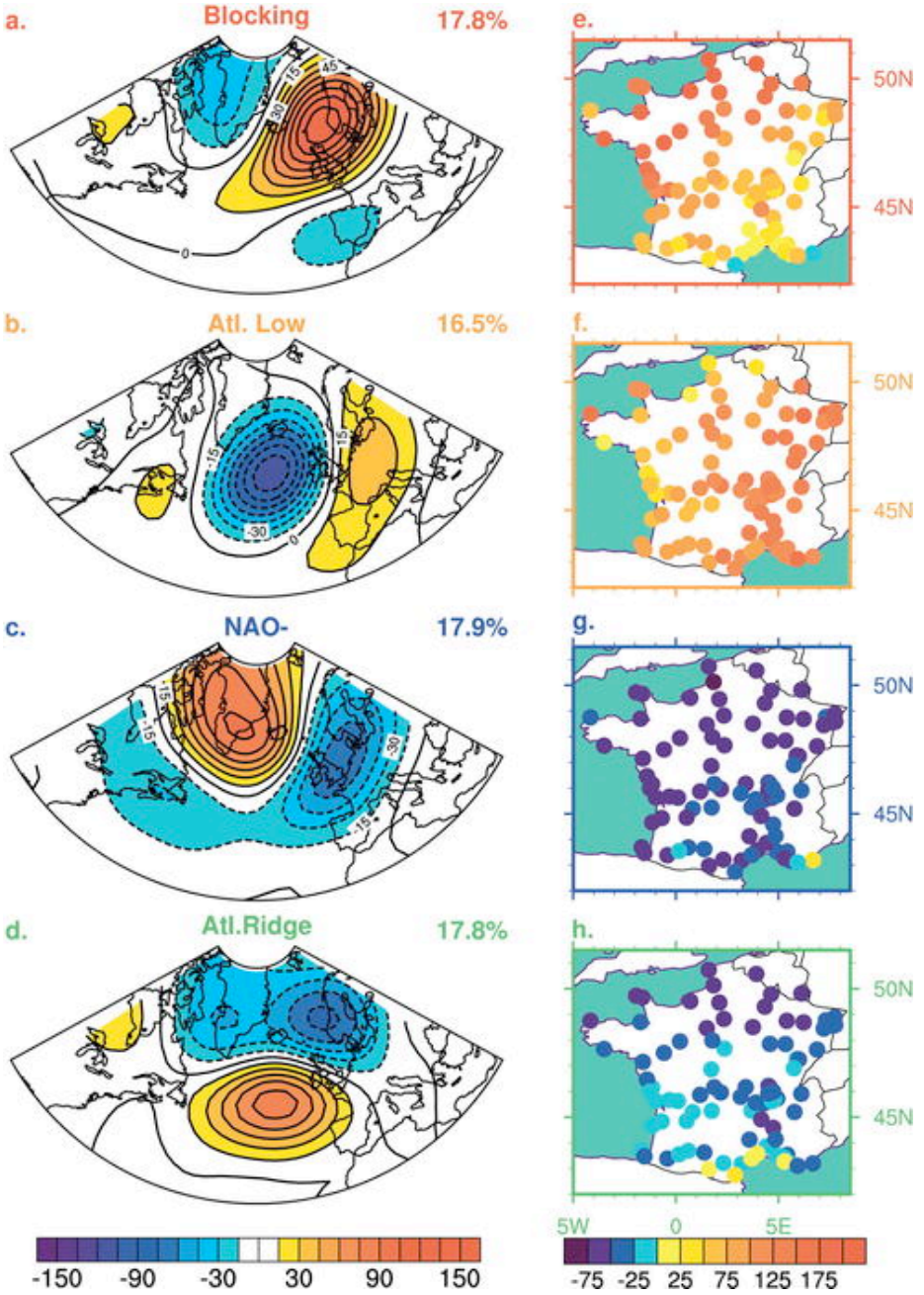

FIG. 1. (a)–(d) Summer Z500 weather regimes computed over the North Atlantic–European sector from 1950 to 2003. Contour interval is 15 m. (e)–(h) Relative changes (%) in the frequency of extreme warm days for each individual regime. Color interval is 25% from −100% to 200%, and red above that (max equal to 233%). As an example, 100% corresponds here to the multiplication by 2 of the likelihood for extreme warm days to occur.

Anticyclonic regimes have a higher frequency of occurrence in the heat-wave summers.

	Warm regimes			Cold regimes		
Year (temperature)	Blocking	Atl.Low	Sum	NAO−	Atl.Ridge	Sum
Mean occurrence	18	17	35	18	18	36
2003 (+3.21°C)	20	40	60	15	0	15
1976 (+2.18°C)	37	25	62	0	7	7
1950 (+1.99°C)	0	45	45	18	10	28
1983 (+1.39°C)	43	0	43	0	32	32
1994 (+1.02°C)	24	32	56	0	14	14

Percentage of occurrence for each regime for the five warmest summers in France since 1950. The selection of the year is simply based on the five highest anomalous temperatures averaged over the 91 weather stations for JJA (anomalous values given in parentheses with the year). Sums for warm regimes (Blocking + Atl.Low) and cold regimes (NAO– + Atl.Ridge) are provided in the fourth and last columns, respectively.

The problem of predicting a heatwave can therefore be linked to the problem of predicting weather regimes frequency.

<u>The main regime dynamics is internal</u> (many authors, e.g. Micheal Ghil)

But also, there are external forcings that influence their:
probability. Of these we can mention:

1. The effect of SST

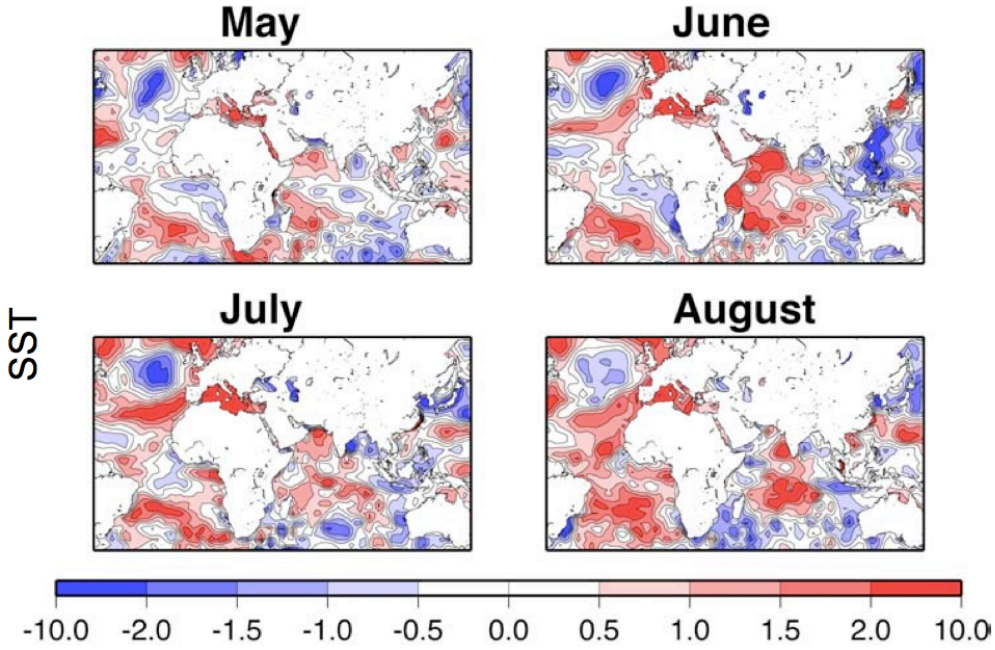

Black and Sutton 2004

2. The effect of tropical forcing →

2. The effect of tropical forcing

Increased convective activity in the tropical Atlantic region increases the frequency of anticyclonic regimes.

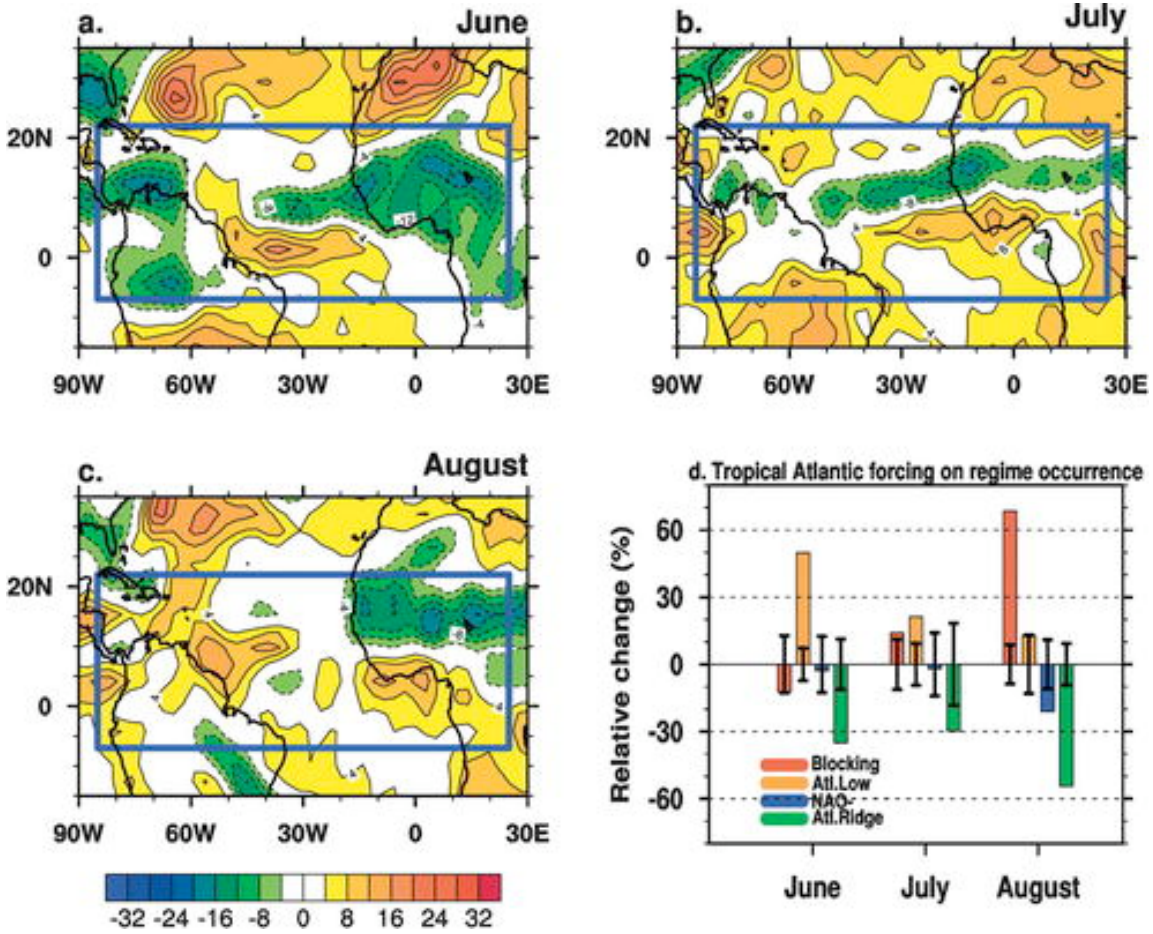

FIG. 2. (a)–(c) Observed OLR anomalies. Anomalies (the base period for climatology is 1979–95) are computed for the three summer months taken individually. Greenish (orange) colors correspond to enhanced convective activity or wetter (drier) conditions. The blue box shows the tropical domain where the diabatic heating perturbations are estimated from OLR anomalies and further imposed in model experiments as detailed subsequently. Contour interval is 4 W m^{-2}. (d) Relative change (%) of occurrence of the four regimes due to the prescribed tropical forcing in the atmospheric model. We tested that the relative changes are not dependent on the choice of the 40-yr period for the control simulation. As a final estimate of the significance, the error bars indicate the range of uncertainty due to internal atmospheric variability as given by one standard deviation of the within-ensemble variability (Farrara et al. 2000).

(Cassou et al 2005 J. Clim)

The effect of global and mediterranean SST (Feudale and Shukla 2007, *GRL*)

Twin GCM simulations forced with global and mediterranean observed SST.

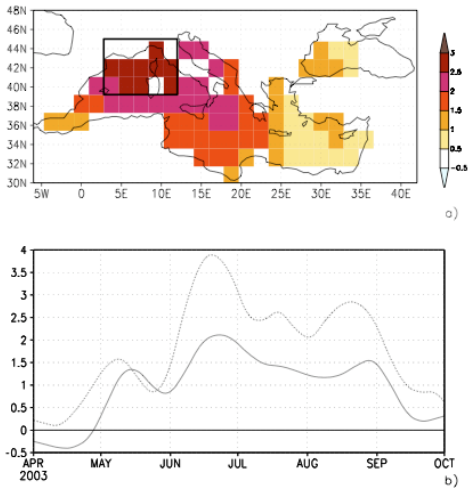

Figure 1. (a) JJA 2003 SST anomaly (°C) in the Mediterranean basin and Black Sea. The rectangle in the region (2.8°E–12°E, 39.2°N–45°N) shows the area with the highest SST anomalies. (b) Time-series of SST anomaly (°C) for the Mediterranean and Black Sea (solid) and for the rectangle shown in Figure 1a (dashed).

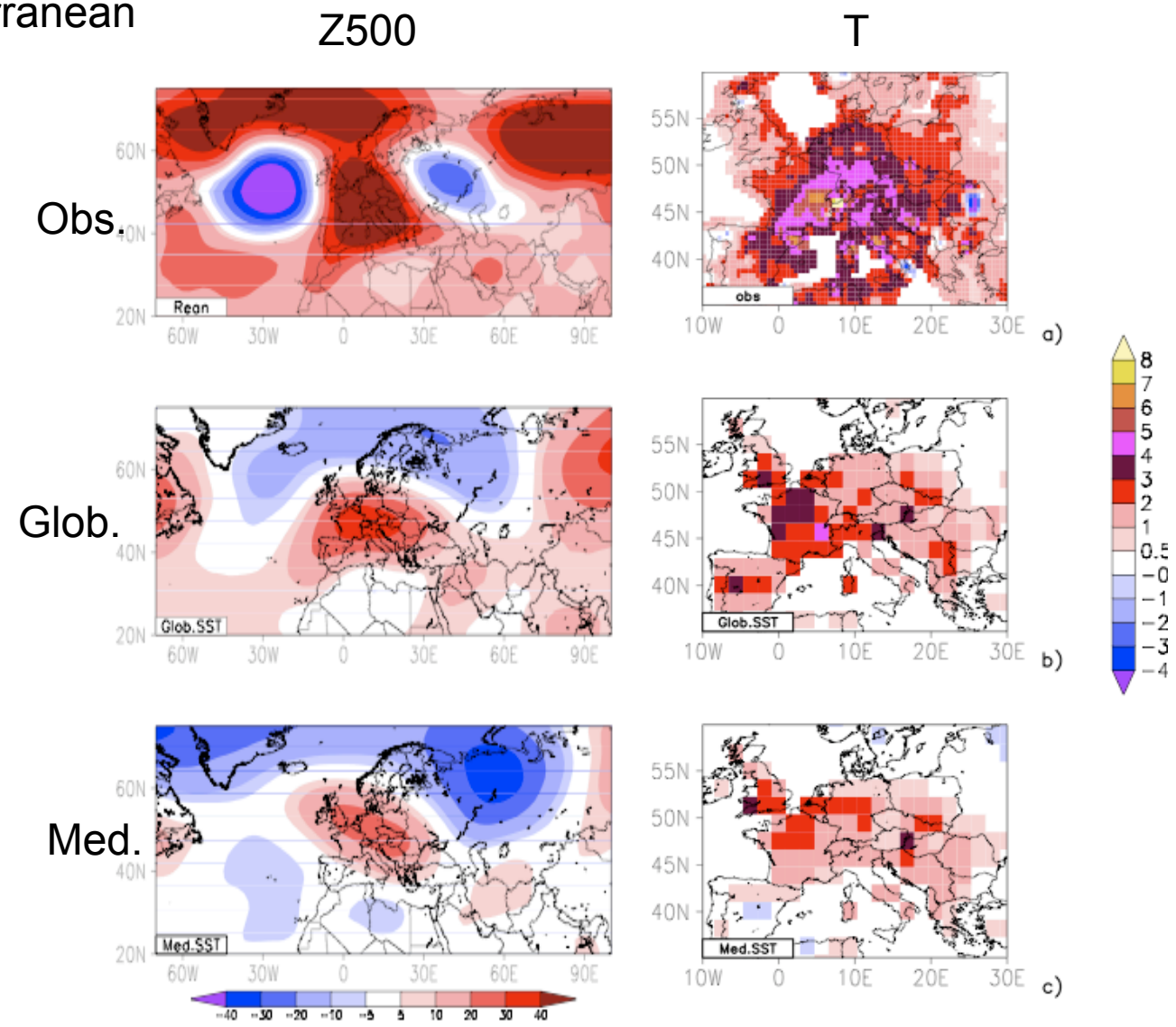

But the change in frequency of the regimes may not be telling the whole story.

The « climate », (i.e. the mean) of a given variable can be seen as the result of succession of weather regimes.

If $\overline{X}_n$ are the composites of the variable, linked to a given regime, The mean climate can be decomposed like this:

$$\overline{x} = \sum_{n=1}^{N} f_n \overline{X}_n$$

Example, temperature in France:

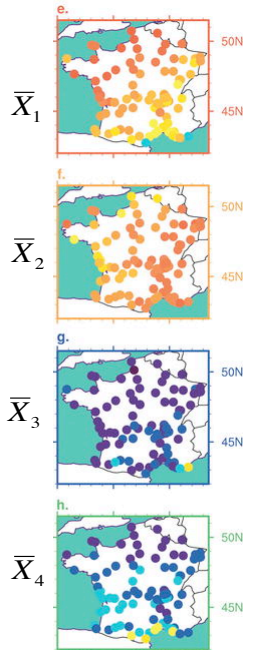

Decomposition of an anomaly

An anomaly ca be decomposed into change in weather regime frequency:

$$\hat{x} - \overline{x} = \sum_{n=1}^{N} (\hat{f}_n - f_n)\overline{X}_n + R$$

If a change of regime frequency is the only cause of the anomaly, the residual is zero. The complete decomposition is:

$$\hat{x} - \overline{x} = \sum_{i=1}^{k} (\hat{f}_i - f_i)\overline{X}_i + \sum_{i=1}^{k} \hat{f}_i(\hat{X}_i - \overline{X}_i)$$

Is this decomposition good in the case of the Heatwave?

We will now check the anomaly decomposition on a 57 year dataset of station measurement in Europe for temperature and precipitation frequency.

We select the 10 hottest years:

Figure 1: a) Summertime (JJA) anomaly composites (°C) over the hottest 10 summers in the 1948-2004 period; b) same as a) but for JJA precipitation frequency (%). Stations where the anomaly is significant at the 90% level are marked by a black bullet;

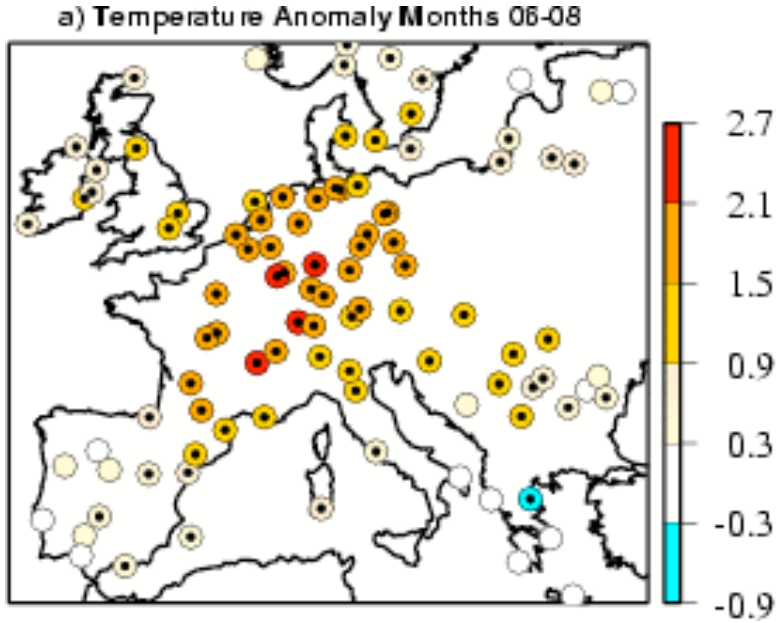

Vautard et al 2007. *GRL*

Hot summers:

1950
1952
1959
1964
1976
1983
1992
1994
1995
2003

Reconstructed anomalies of Tmax and precipitation frequency.

<u>The reconstruction is always too cold and too wet.</u>

Temperature

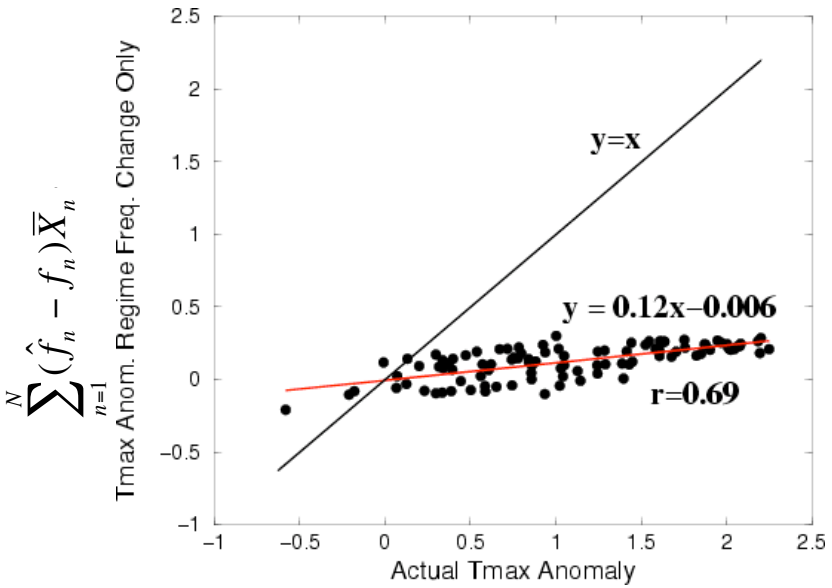

Precipitation

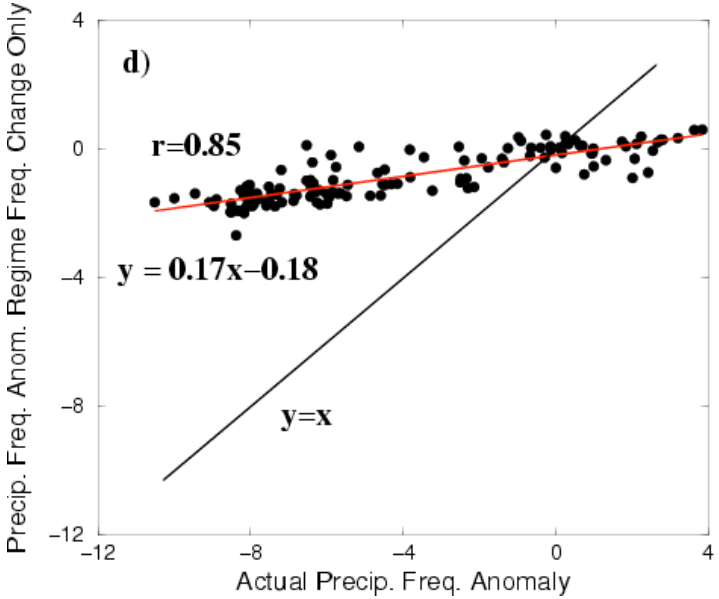

c) Average anomalies, over the hottest 10 years, of maximal daily temperatures that would obtain by a sole change in the frequencies of summertime weather regimes [Cassou et al., 2005], as a function of the corresponding actual average anomalies. Each point corresponds to a station. See the methods section for details of calculation; d) Same as c) for precipitation frequencies.

A reconstruction by analogues does not explain the increase in temperature and the decrease of precipitation events.

Expecially since the 80's

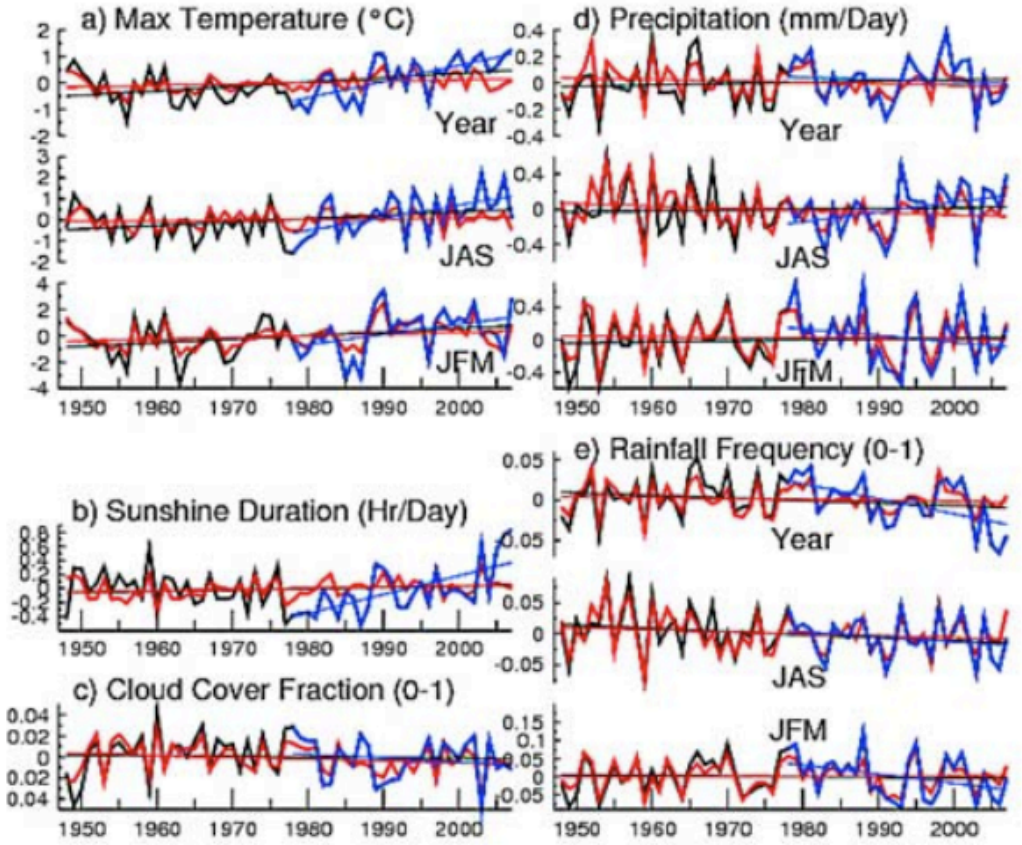

Figure 1. Time evolution of the annual or seasonal average, over all available European stations, of observed (black curves for the earliest 30 years and blue curves for the latest 30 years) or constructed (red curve) anomalies, together with linear regression lines; (a) maximal temperature (°C) for (top) annual average, (middle) summer (JAS) average, and (bottom) winter average; (b) sunshine duration (h/day); (c) cloud cover (0–1 fraction); (d) as in Figure 1a for precipitation amounts (mm/day); (e) as in Figure 1a for rainfall frequency (0–1 fraction).

Vautard and Yiou GRL 2009

There is another mechanism that must be responsible for the strong temperature and precipitation anomalies. A good candidate: **SOIL MOISTURE.**

Heatwaves have been observed to be preceeded by precipitation deficit (Huang and Van den Dool 1992 J. Clim.

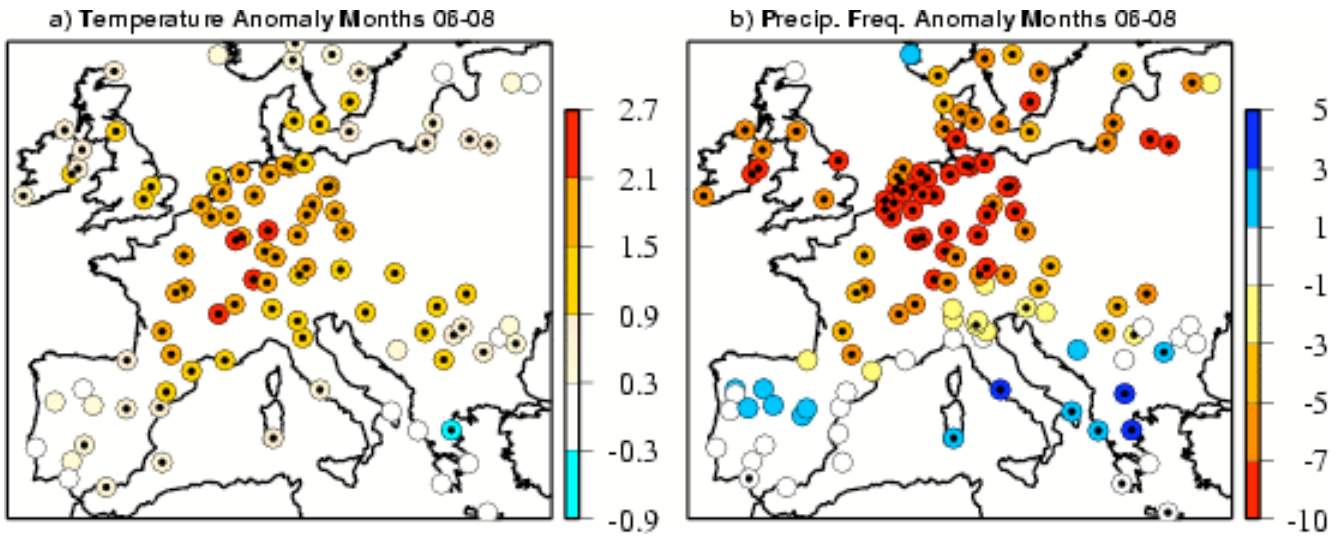

Figure 1: a) Summertime (JJA) anomaly composites (°C) over the hottest 10 summers in the 1948-2004 period; b) same as a) but for JJA precipitation frequency (%). Stations where the anomaly is significant at the 90% level are marked by a black bullet;

Soil moisture controls the energy balance between the earth surface and the atmosphere by modulating sensible and latent (evaporation) heat fluxes.

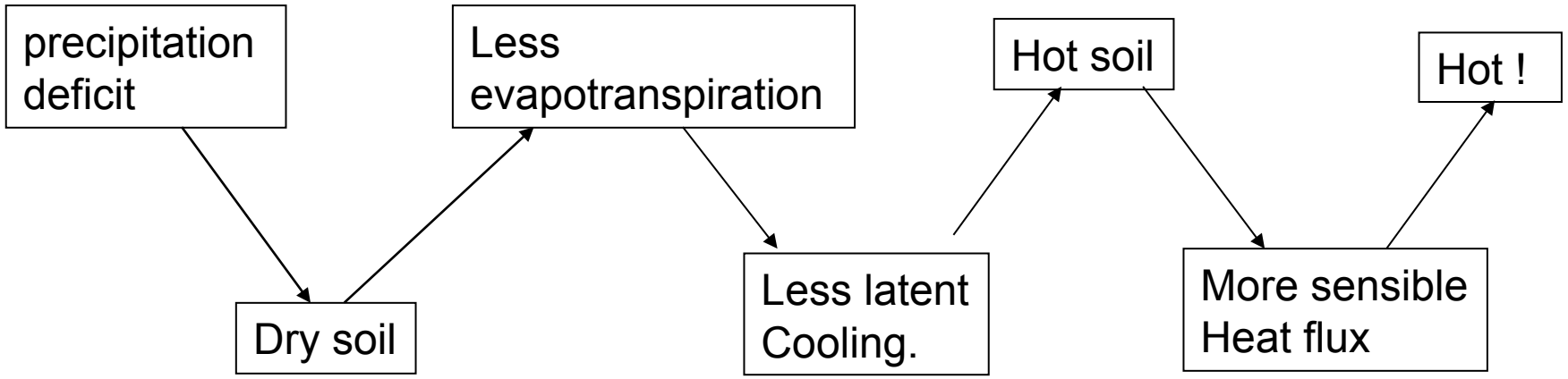

An old example

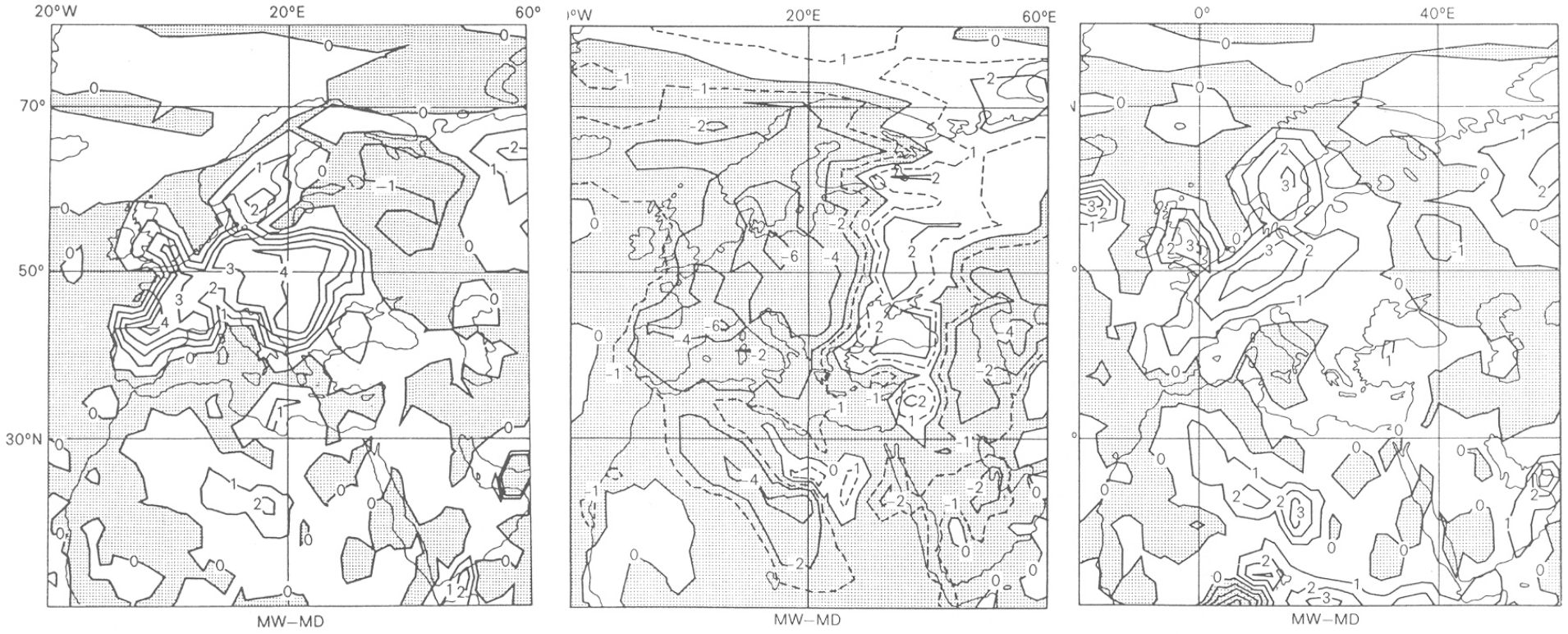

Evaporation

Temperature

Precipitation

Response of the UKMO GCM to prescribed values of soil moisture (Wet – Dry)

Rowntree and Bolton (1983)

Soil moisture controls the energy balance between the earth surface and the atmosphere by modulating sensible and latent (evaporation) heat fluxes.

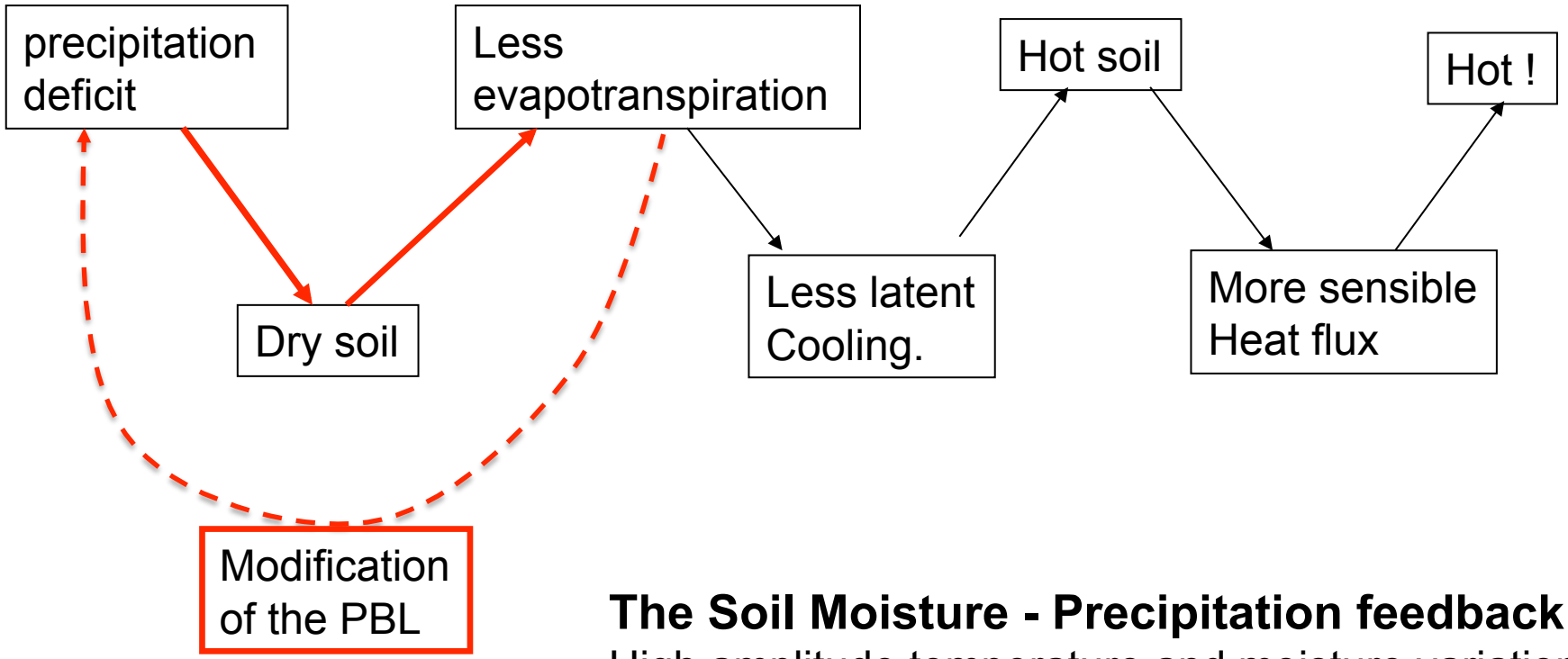

The Soil Moisture - Precipitation feedback

High amplitude temperature and moisture variation are maintained by a feedback between soil moisture and precipitation (Schär et al 1999).

A more recent example from the group of Christophe Schär in Zurich

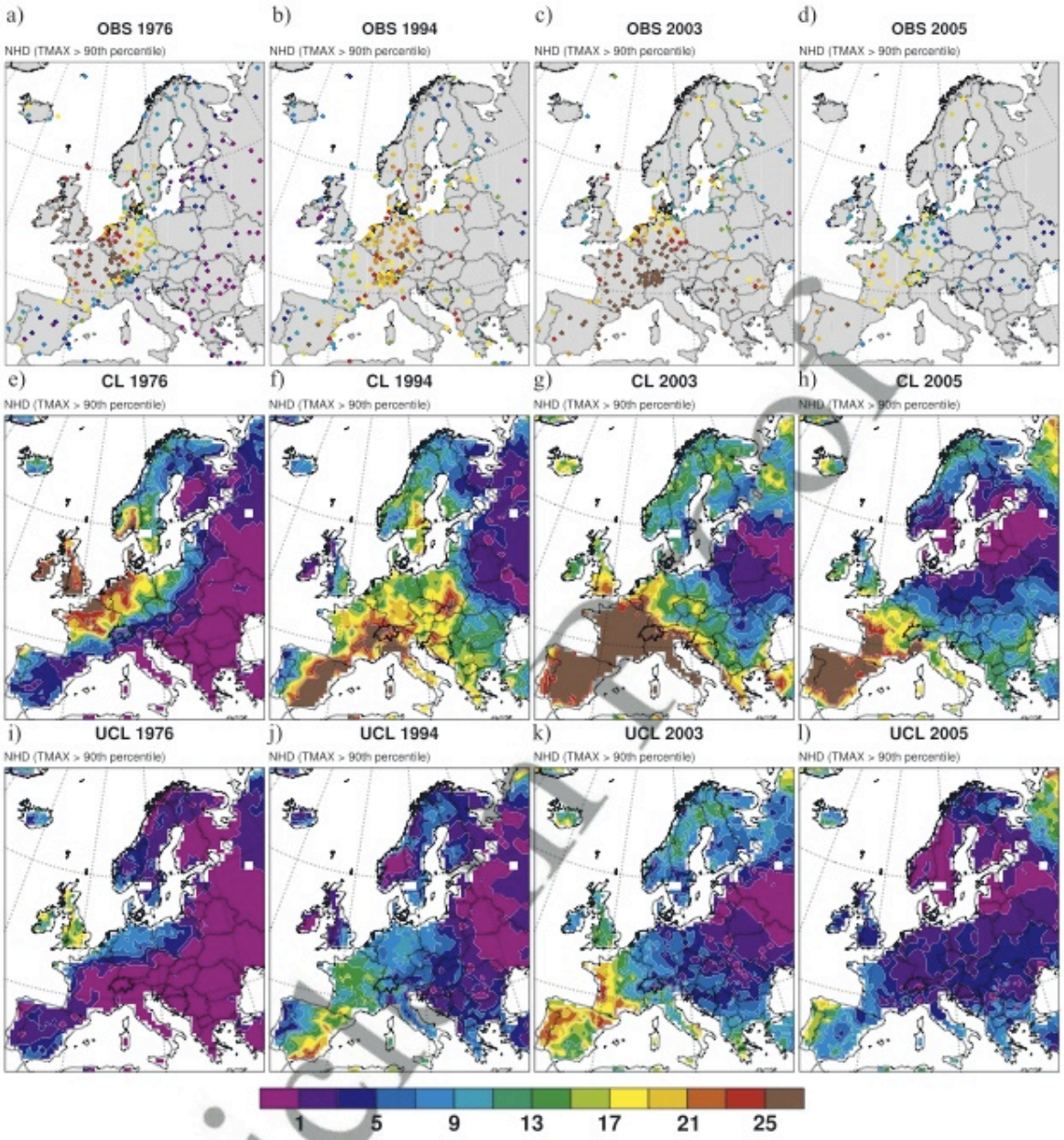

Fischer et al 2007 - GRL

Figure 2. Number of hot days (NHD) derived from (a–d) observed ECAD daily maximum temperature series, and (e–h) the simulations with (CL) and (i–l) without land-atmosphere coupling (UCL) during the summers (JJA) 1976, 1994, 2003, and 2005.

Regional GCM integrations of the year 2003, with prescribred soil moisture anomalies

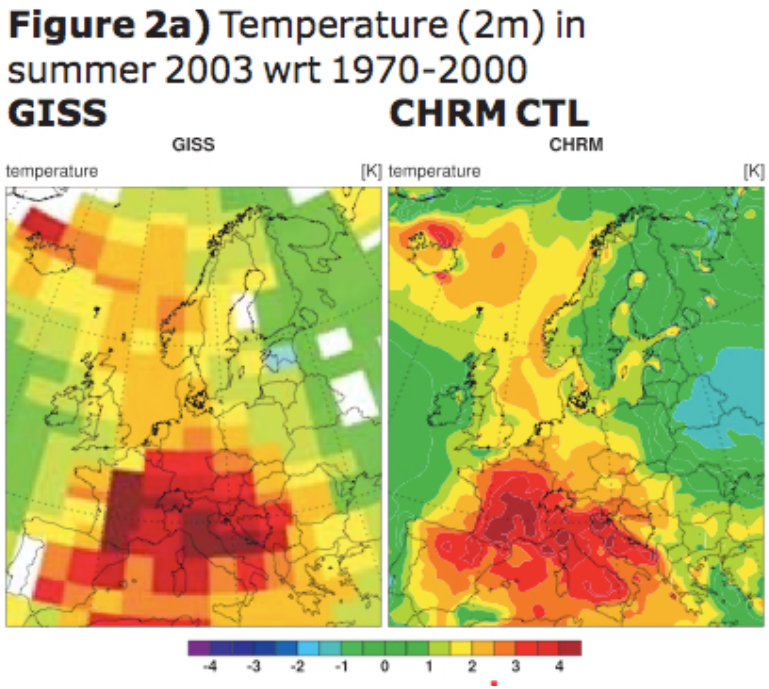

Control integrations

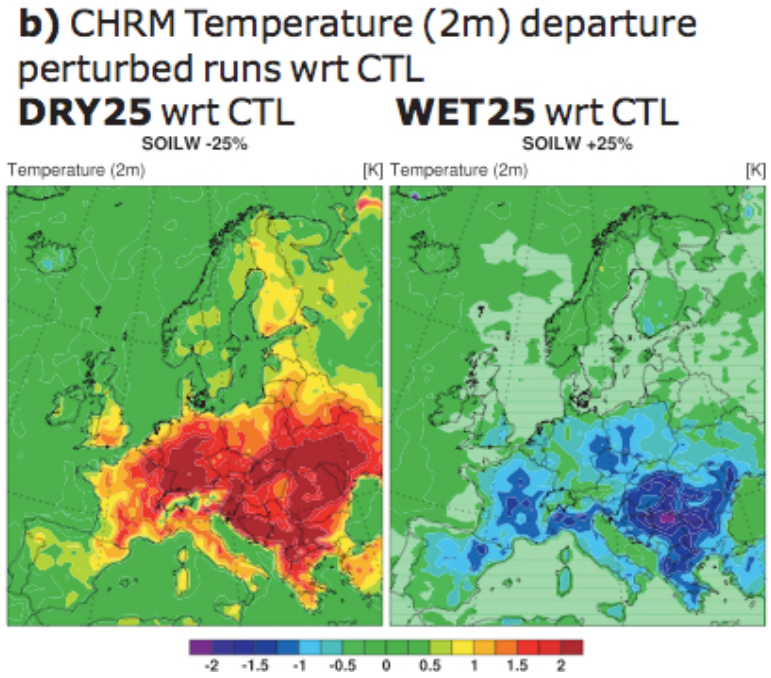

Perturbed integrations

Fischer et al 2005

Time evolution integrated over France

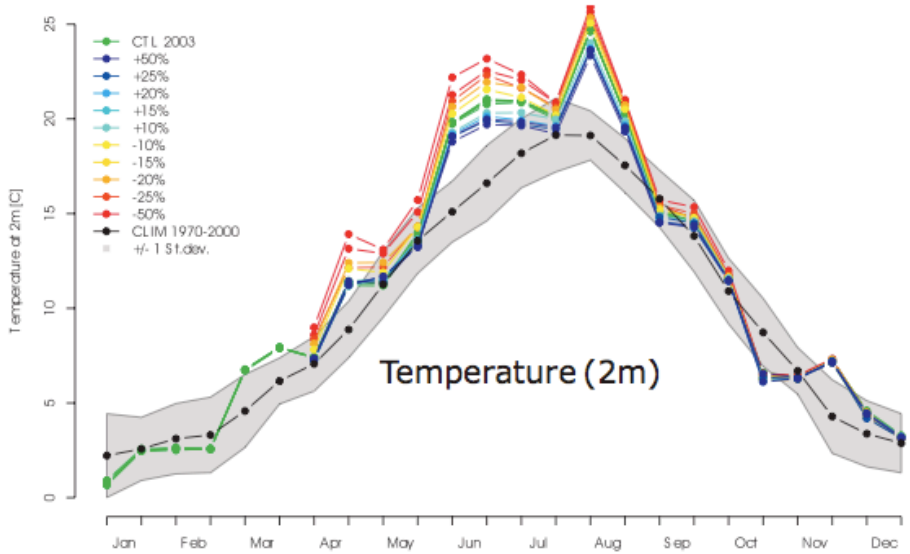

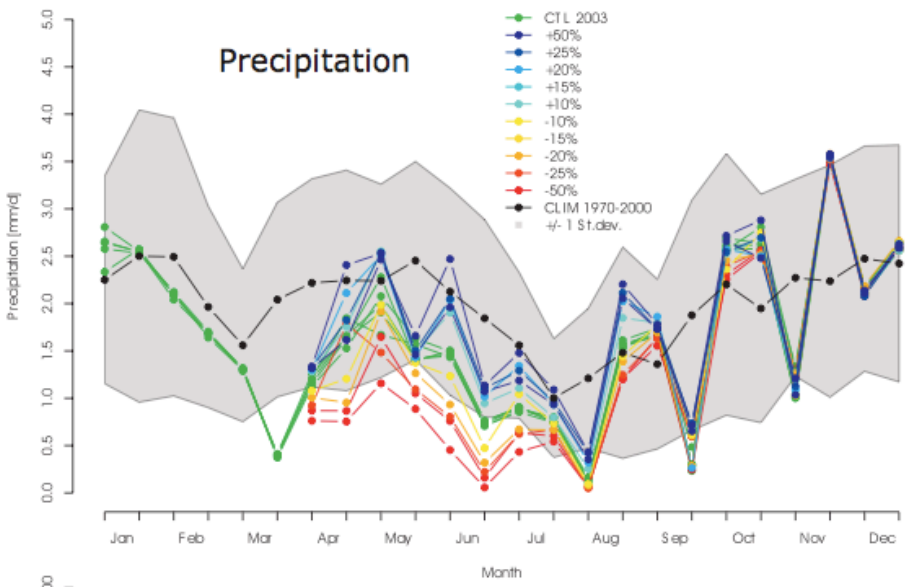

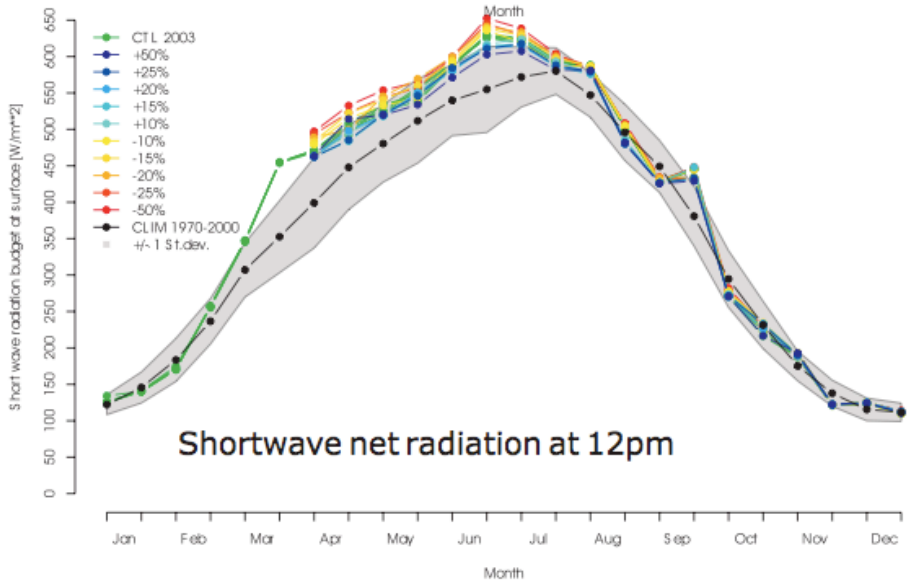

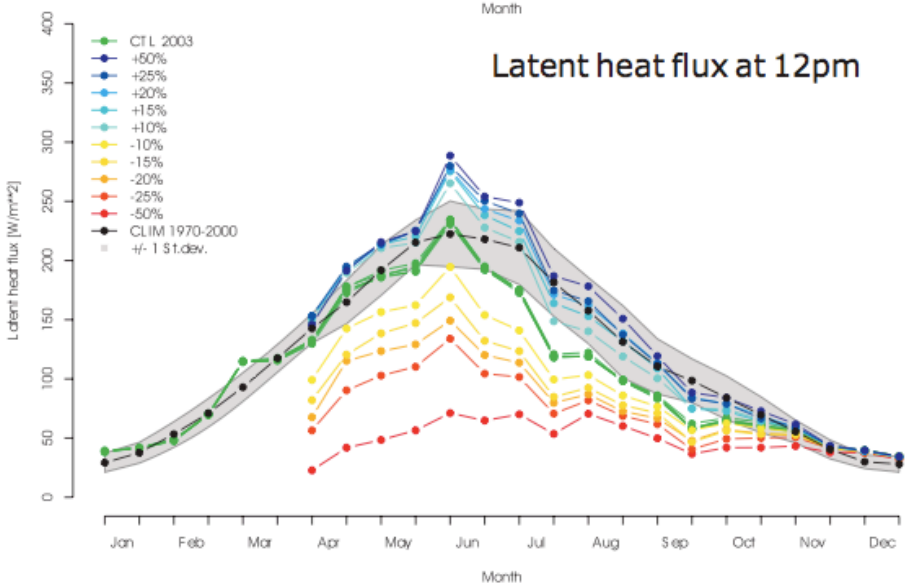

Fischer et al 2005

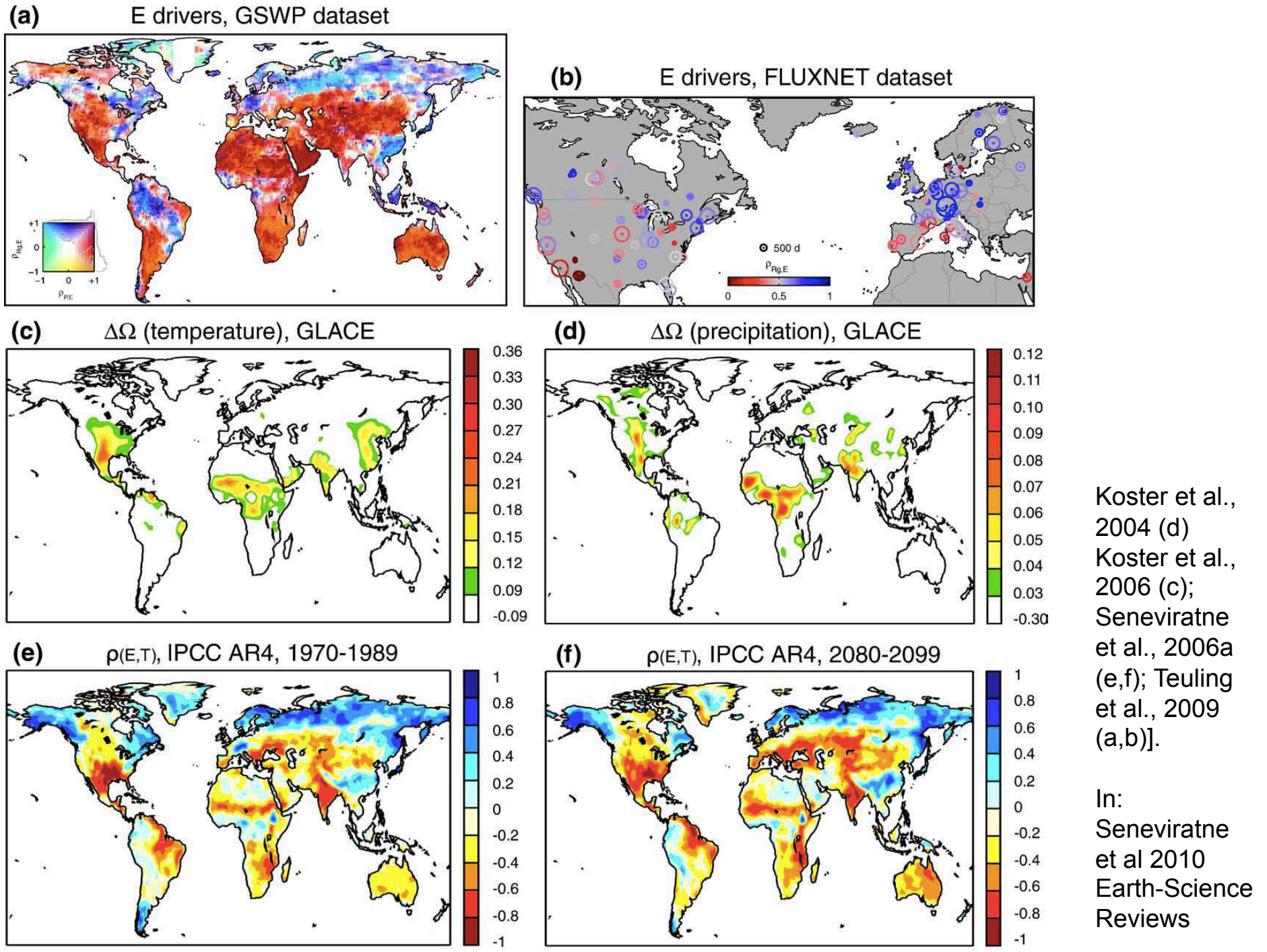

Koster et al., 2004 (d) Koster et al., 2006 (c); Seneviratne et al., 2006a (e,f); Teuling et al., 2009 (a,b)].

In: Seneviratne et al 2010 Earth-Science Reviews

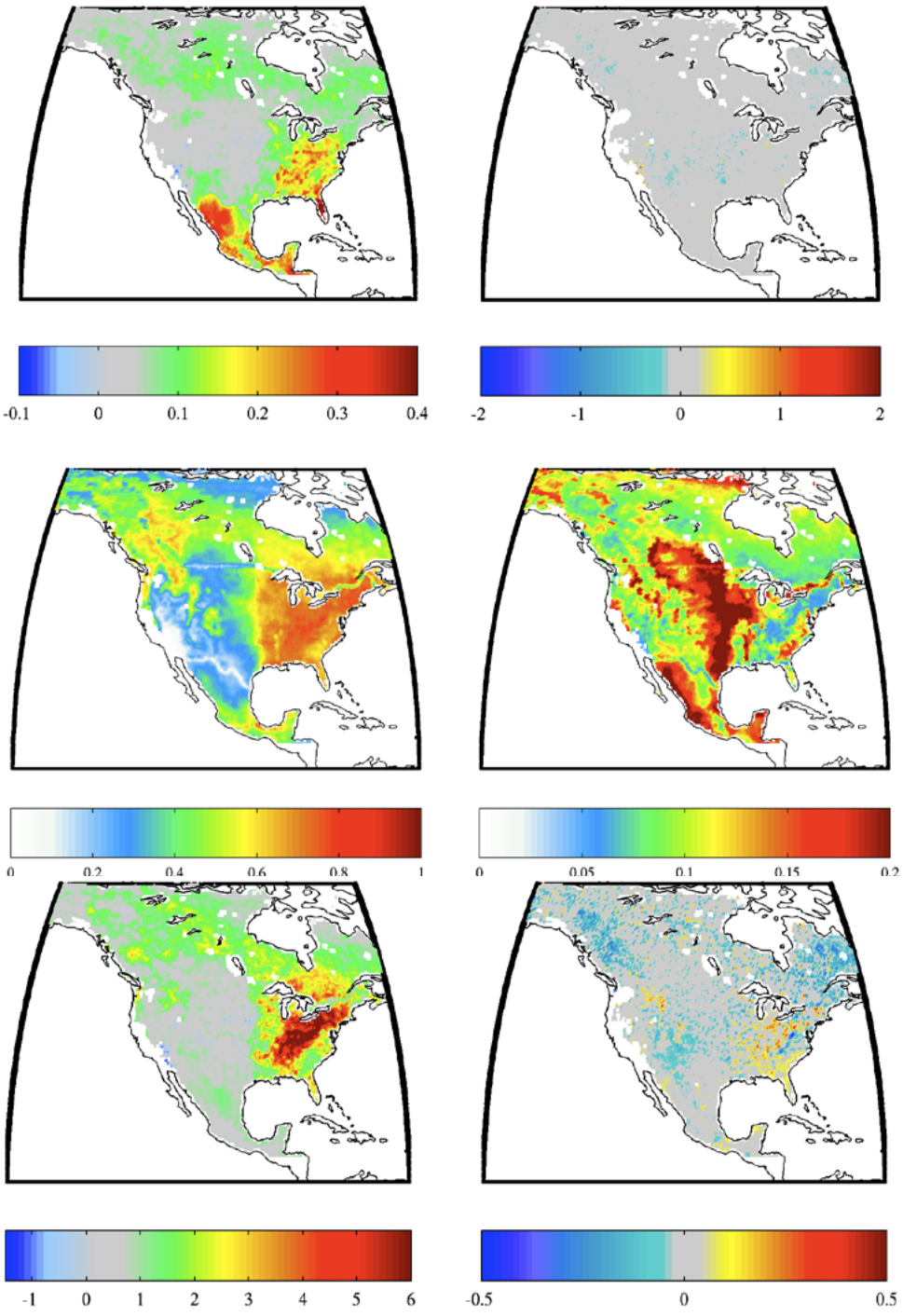

$2\sigma_{EF}\frac{\partial}{\partial EF}E(r)$ $2\sigma_{EF}\frac{\partial}{\partial EF}\Gamma(r)$

$\overline{EF}$ σ_{EF}

$\frac{\overline{EF}}{\Gamma(r)}\frac{\partial}{\partial EF}\Gamma(r)$ $\frac{\overline{EF}}{E(r)}\frac{\partial}{\partial EF}E(r)$

Findell et al 2010, Nature (subm).

Little conclusions - 1

1. Soil moisture in important

2. There are “hot spots” of land-climate interaction

3. Their identification is still difficult

4. The mechanisms of soil moisture – precipitation interaction are still unclear
   3.1 there is evidence that SM increases the frequency of rain but not the intensity of rain events.

3. An idealized study

At this point, we really need to study the dynamics of soil water, and its interaction with the atmosphere. This means studying convection, water and heat fluxes, the physics of evaporation, the physiology of plants.

Water balance on a layer of soil

$$\frac{\partial Q_s}{\partial t} = P - E - R - L$$

…water for one week…

In a hot summer day, a mature tree can evaporate 2000 liters of water!

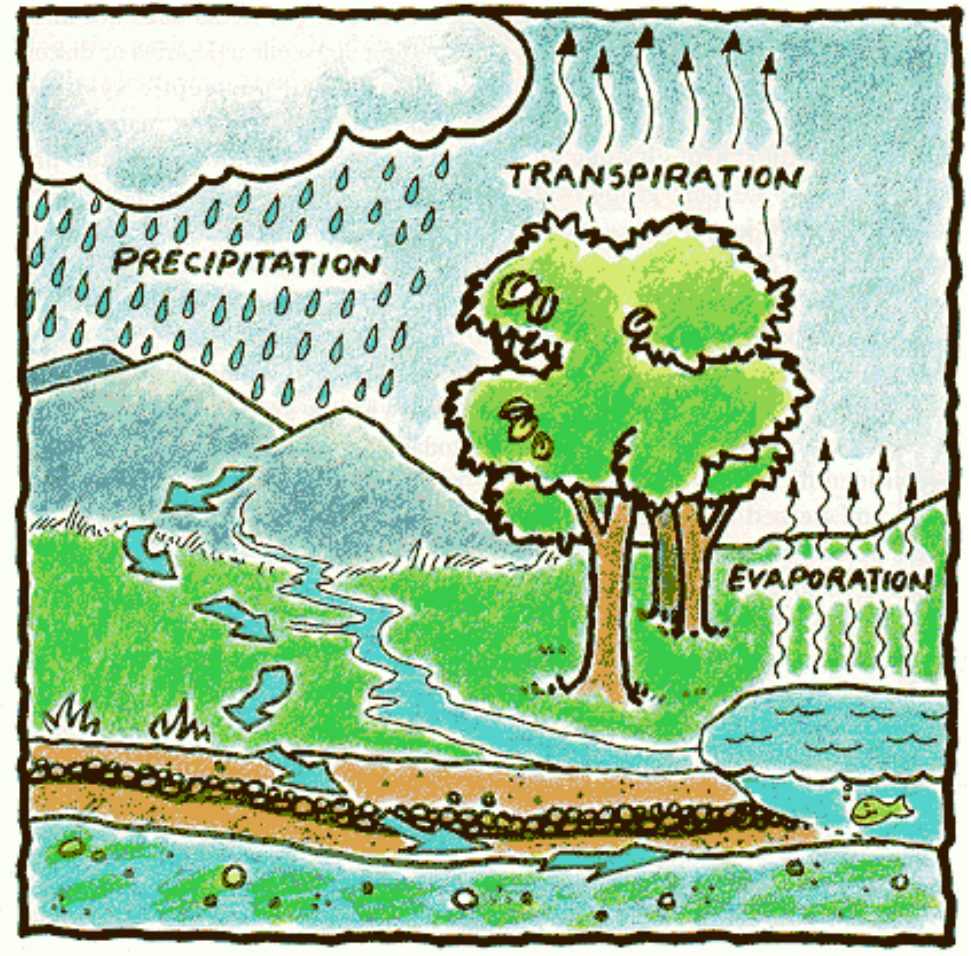

Box model description (D'Andrea et al 2006 *GRL*)

Evaporation Rate

$$\begin{cases} E' = 0 & for\ q_s \le q_h \\ E' = \dfrac{q_s - q_h}{q_w - q_h} E_w & for\ q_h \le q_s \le q_w \\ E' = E_w + \dfrac{q_s - q_w}{q^* - q_w}\left(E_{Max} - E_w\right) & for\ q_w \le q_s \le q^* \\ E' = E_{Max} & for\ q_s \ge q^* \end{cases}$$

$q_h = 0.14$ Hygroscopic point

$q_w = 0.18$ Wilting point

$q^* = 0.56$ Maximum Plant Efficiency

$E_w = 1.0610^{-6} \ \dfrac{Kg}{m^2 s}$

$E'_{Max} = 6 \ 10^{-5} \ \dfrac{Kg}{m^2 s} \left[\approx 5.2 \dfrac{mm}{d}\right]$

$$E = E' \frac{q_{Sat} - q_a}{q_{Sat}};$$

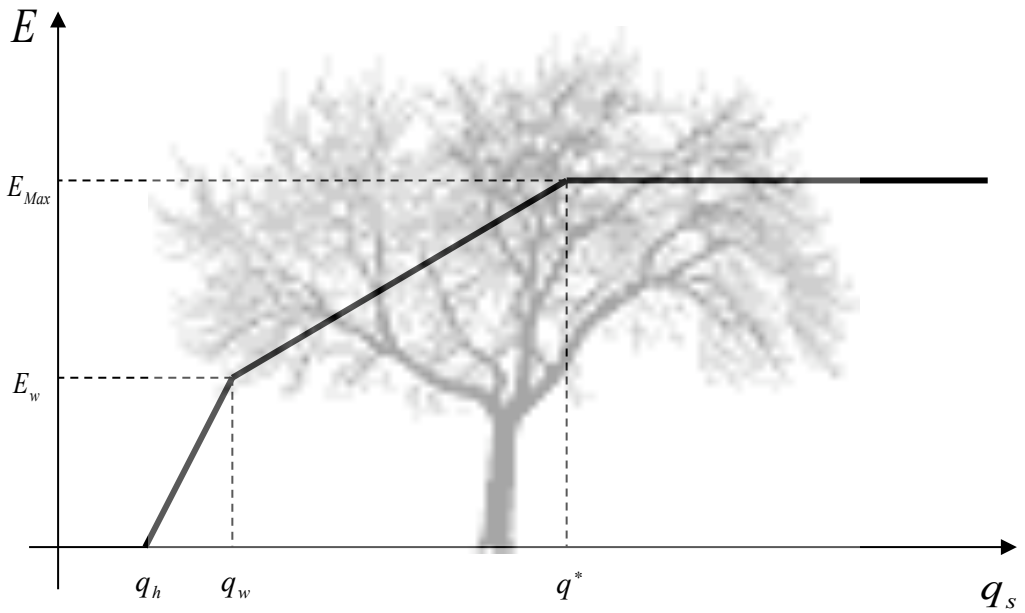

(Laio et al 2001)

Leakage

$$L(q_s) = K_s \frac{e^{k(q_s - q_{fc})} - 1}{e^{k(1 - q_{fc})} - 1}$$ (Laio et al 2001)

$$q_{fc} = 0.56$$

Sensible heat flux

$$Q_s = \rho C_p C_D |\mathbf{u}| (T_s - \theta_a)$$

Precipitation Rate and Runoff (1)

$$P = f \frac{1}{dt} \Delta \tilde{q}_S$$

$$\begin{cases} P' = P & for\ P \le \frac{q_0 - q_s}{dt} \\ P' = \frac{q_0 - q_s}{dt} & for\ P \ge \frac{q_0 - q_s}{dt} \end{cases}$$

Convection

$$if\ \theta_e - \theta_e^* \geq 0$$

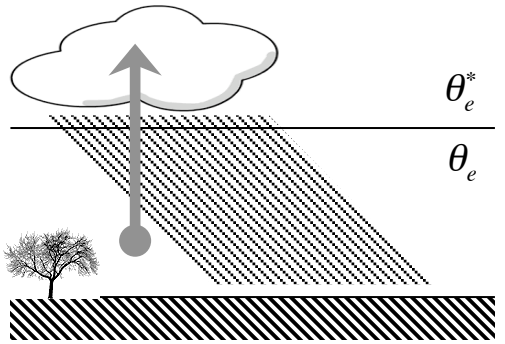

$$\begin{cases} \Delta\tilde{\theta}_a = \dfrac{\theta_e - \theta_e^*}{1 + \dfrac{L_e}{c_p} q_{Rel}\delta q_s} & (cooling) \\ \Delta\tilde{q}_a = q_{Rel}\delta q_s \Delta\tilde{\theta}_a & (drying) \end{cases}$$

Where: $\delta q_{sat} = \dfrac{\partial q_{Sat}}{\partial T_a}$ *and* $q_{Sat} = q_0 e^{-0.622\frac{L_e}{c_p}\left(\frac{1}{T_a} - \frac{1}{273.15}\right)}$

$$q_{Rel} = \frac{q_a}{q_{Sat}}$$

The above formulas for cooling and drying are obtained using the reduction of enthalpy and conserving relative humidity:

$$\Delta\tilde{\theta}_a + \frac{L_e}{c_p}\Delta\tilde{q}_a = \theta_e - \theta_e^* \quad \text{(enthalpy variation)}$$

$$q_{Rel}\delta q_s \Delta\tilde{\theta}_a = \Delta\tilde{q}_a \quad \text{(first order conservation of relative humidity)}$$

Reminder:

$$\theta_e = \theta_a e^{\frac{L_e q_a}{c_p \theta_a}}$$

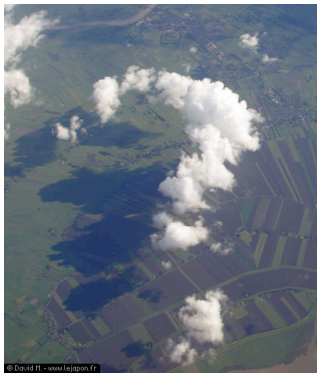

Precipitation Rate and Runoff (2)

$$P = f\frac{1}{dt}\Delta\tilde{q}_a$$

$$\begin{cases} P' = P & for\ P \le \dfrac{1-q_s}{dt} \\ P' = \dfrac{1-q_s}{dt} & for\ P > \dfrac{1-q_s}{dt} \end{cases}$$

Not all the water that is lifted in the free troposphere by convection precipitates.

The fraction of precipitated water depends on the intensity of convection.

f is 0.9 for strong convection and 0.20 for weak convection

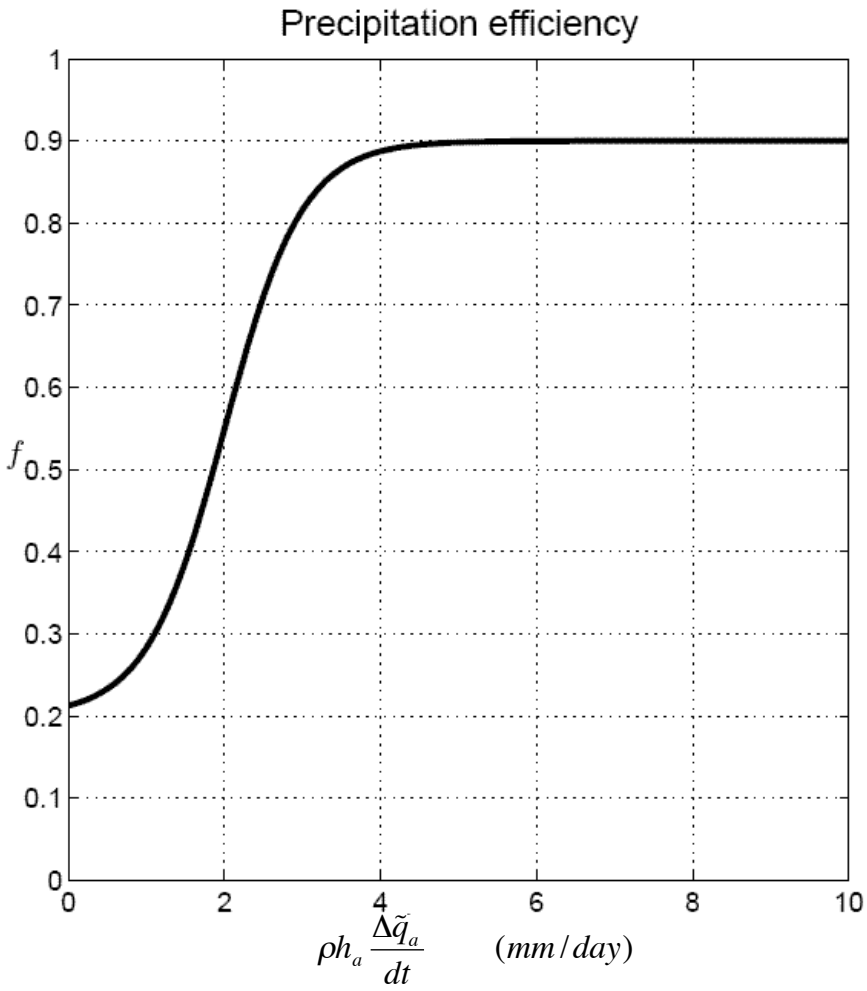

Equilibrium states

As a function of initial soil moisture condition

Some parameter values:

$F_{rad} = 380 \frac{W}{m^2}$ Solar radiation

$\varepsilon = 0.8$ Soil emissivity

$F_q = 1.10^{-8} \frac{Kg}{Kg\,s}$ Lateral flux of humidity

$\theta_e^* = 300\,^oK$ Constant equivalent potential temperature of the free troposphere

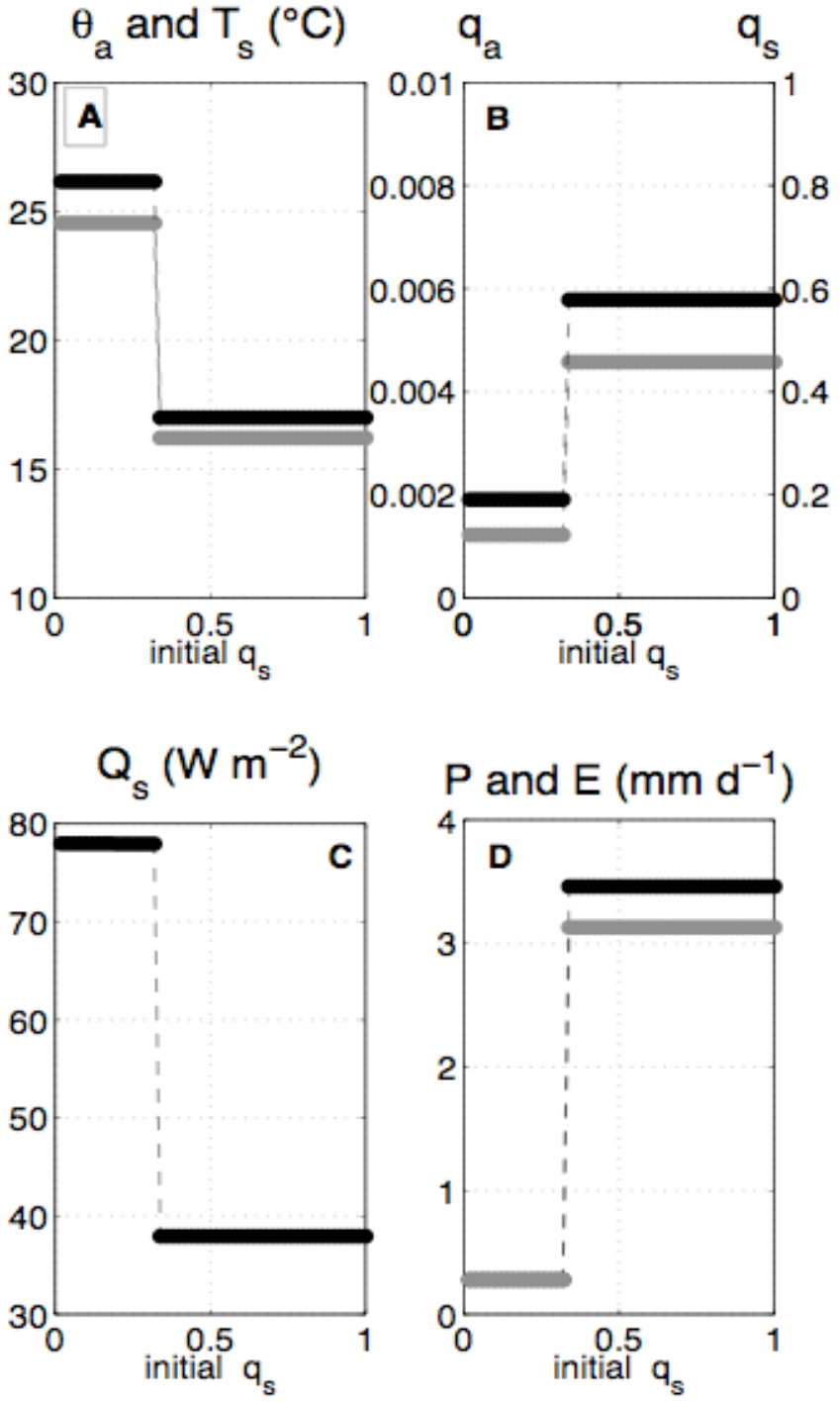

Dependence on the large scale flux convergence

Hysteresis cycle obtained by varying Fq

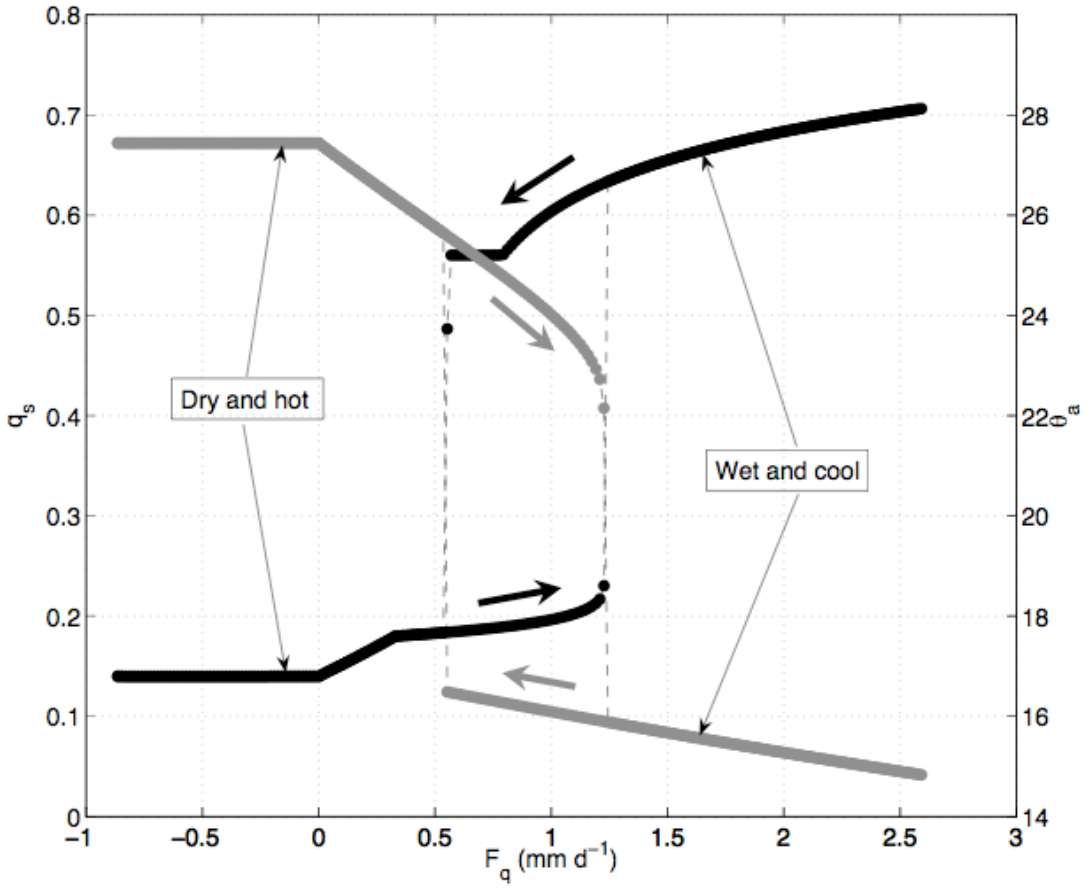

Air temperature

Soil moisture

Stochastically forced integration

Fq is perturbed stochastically every 5 days. Values varying between -1 and 3 mm/day. Flat distribution

Dry and warm regime

Cool and moist regime

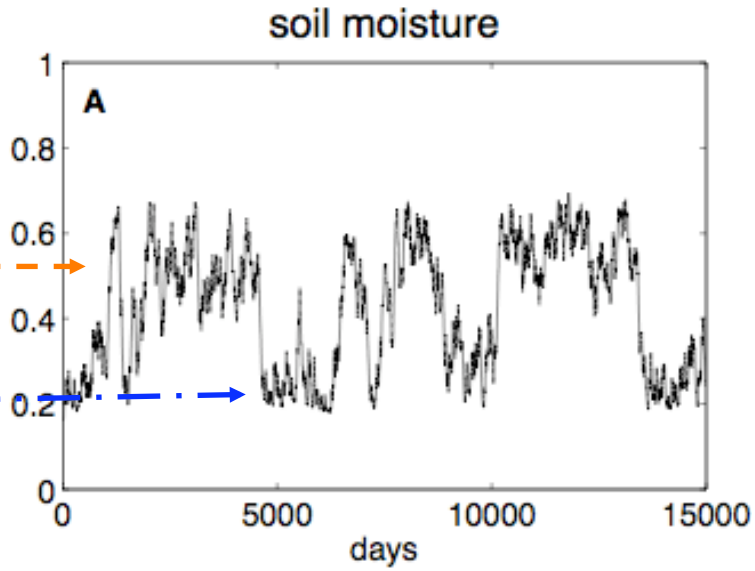

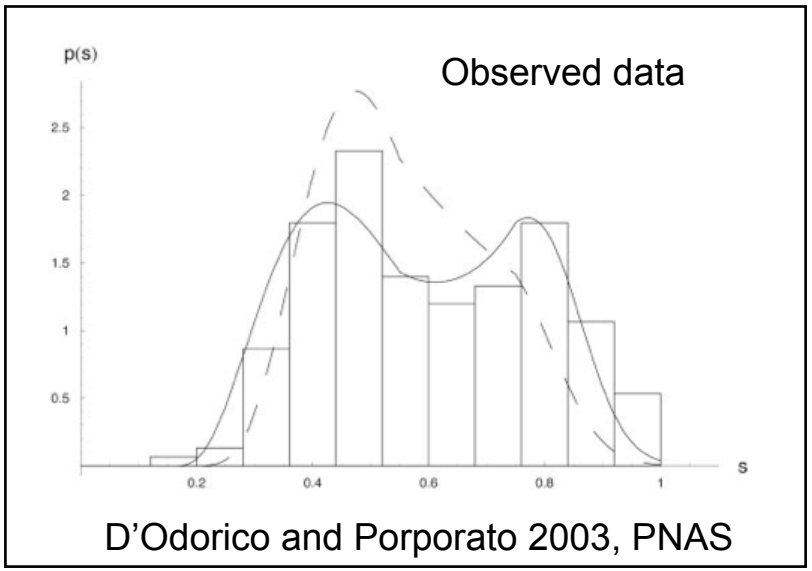

D'Odorico and Porporato 2003, PNAS

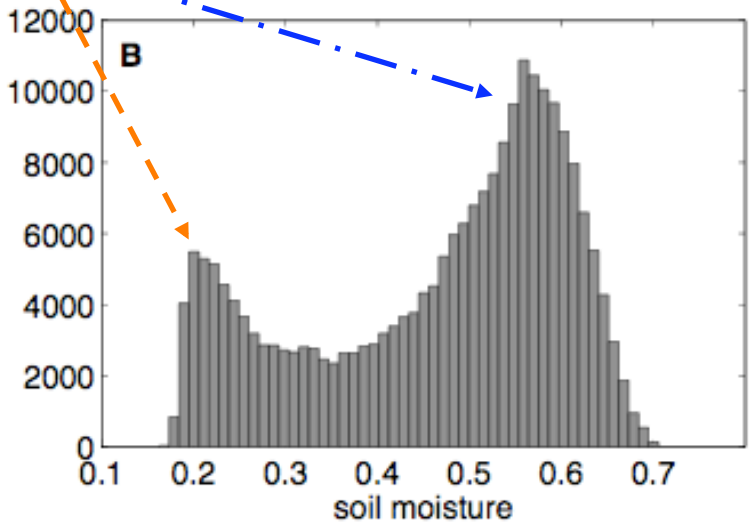

Northward propagation of drought
(Vautard et al 2007, *GRL*)

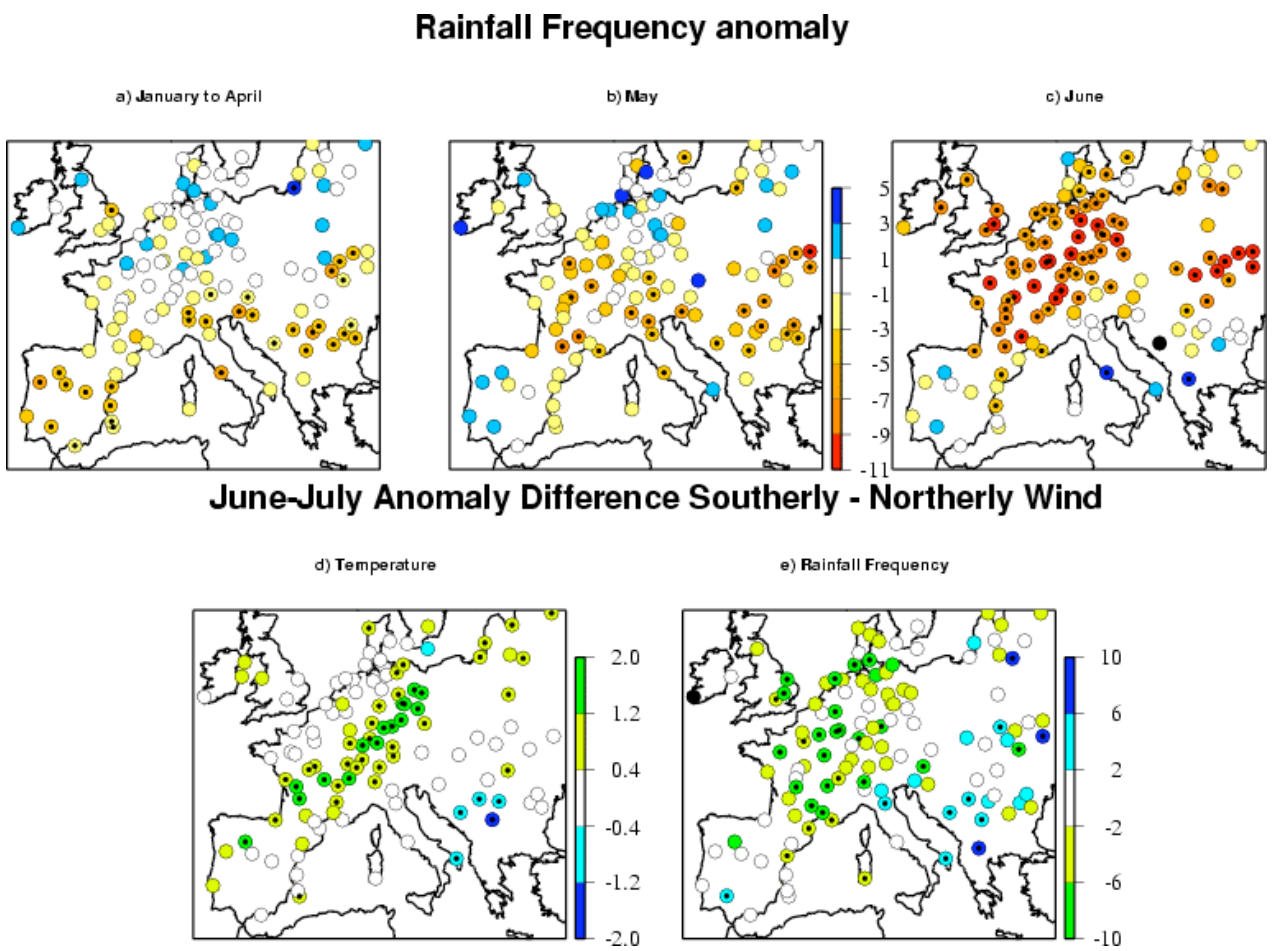

Figure: a) Average rainfall frequency anomaly (% of days) (January–April) for the 10 years containing the hottest summers listed in Table 1 of the Auxiliary Material. The color scale is as in Figure 1b. The figures that would obtain for the winter only (January-march, not shown) or from January to May are rather similar to this one; b) Same as a) for averages of the month of May only; c) Same as a) for June; d) Difference between the early summer (June and July) maximal hot-summer temperature anomalies when southerly wind occurs at the station and that obtained for northerly wind. At each station, days are classified into 2 classes according to the sign of the mean daily surface meridional wind field. The 58-year average maximal temperature is calculated and subtracted from the hot-summer average to obtain mean anomalies. Then the difference between "southerly" and "northerly" mean anomalies is shown in panel d). The figure shows that temperature anomalies, in the 10 hottest summers, are higher in southerly wind conditions than in northerly wind conditions. e) As in d) for rainfall frequency (% of days). Stations where the differences are significant at the 90% level are marked with a black bullet.

Two criteria are necessary for the occurrence of a heat and drought wave:

1. The establishment and persistence of an anticyclonic weather regime
2. A condition of dry soil.

When both criteria are met, the soil moisture - precipitation feedback can maintain large amplitudes of the anomaly.

The initial content in soil water at the beginning of the summer seems to be a crucial parameter. It is more likely that one summer is either in one or the other state and stay there, rather than a transition occur during the season.

Box model description (Baudena et al 2008, WRR)

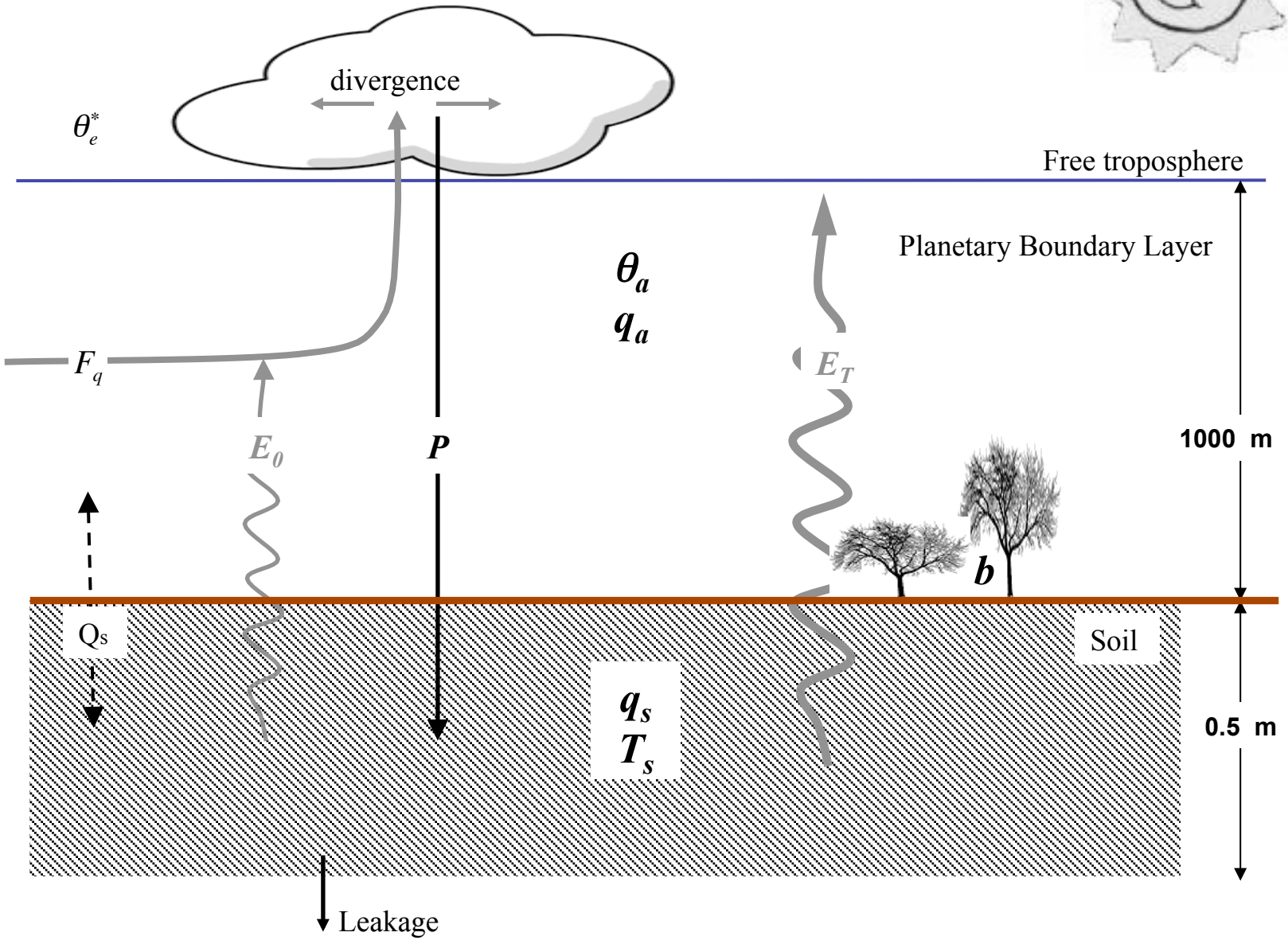

Baudena *et al.*, 2007, in preparation

Box model description (Baudena et al 2008, WRR)

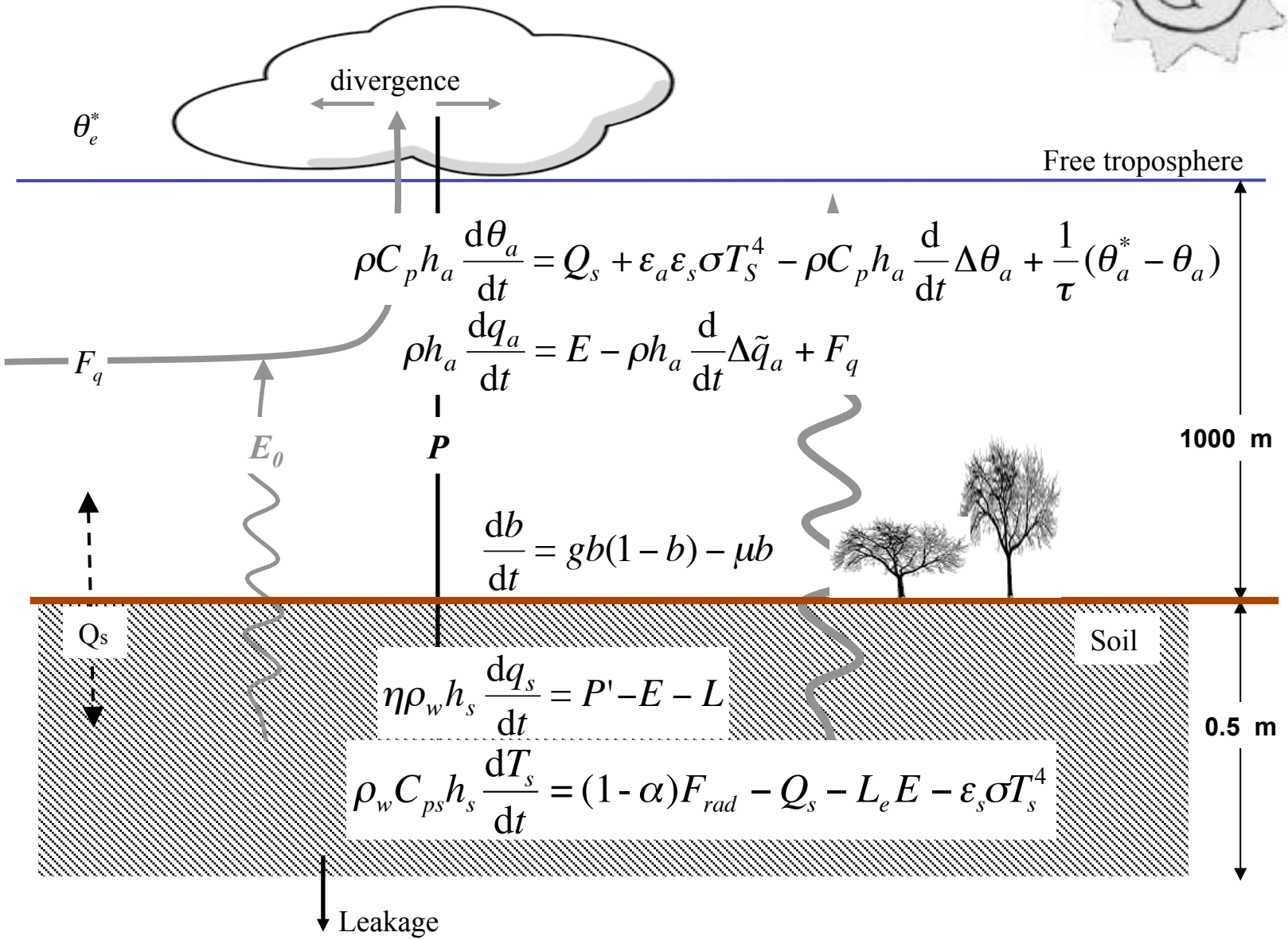

Baudena *et al.*, 2007, in preparation

Baudena *et al.*,

Implicit space logistic equation for vegetation dynamics

b fraction of sites occupied by vegetation

$$\frac{db}{dt} = g(s)b(1-b) - \mu(s)b$$

μ local extinction (mortality) rate

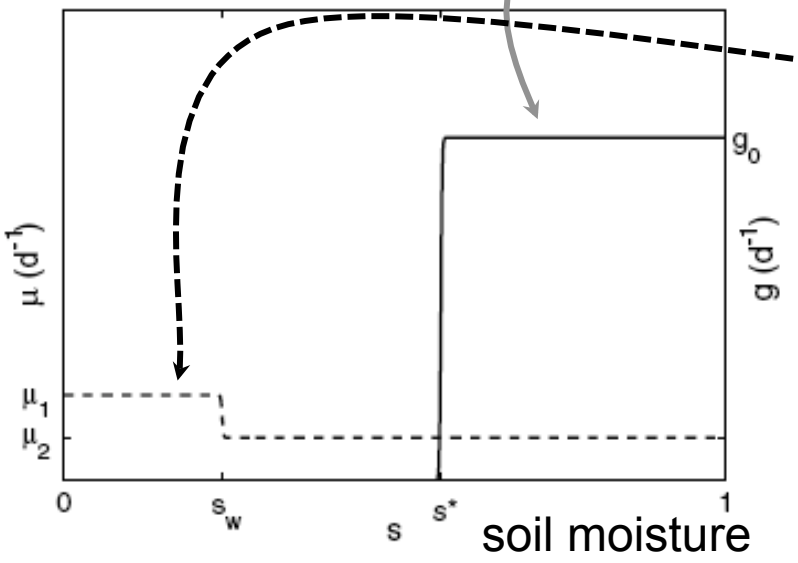

g colonization rate

Baudena *et al.*, Advances in Water Resources, **30** 1320-1328 (2007)

Albedo

$$\alpha = b\alpha_b + (1-b)\alpha_0$$

$$\alpha_0 = 0.35$$
$$\alpha_b = 0.14$$

As in Charney [1975]

Evapotranspiration

$$E = (1-b)E_0(q_s) + bE_T(q_s)$$

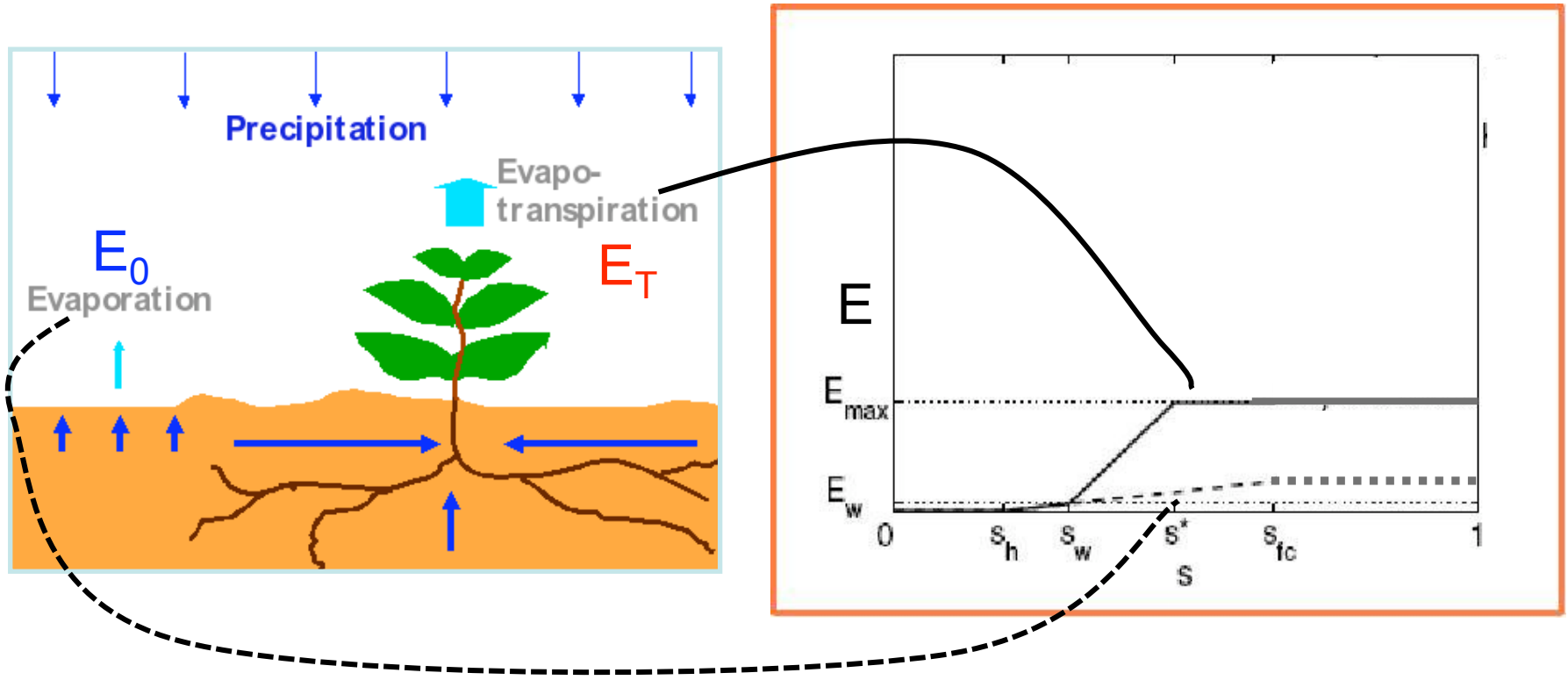

Baudena *et al.*, 2008

2 X 2 experiments

- lateral humidity flux F_q:
  - **constant**
  - **stochastic** (representing synoptic flow variability)
- vegetation:
  - "**natural**" (ability of colonizing new space)
  - "**cultivated**" (higher sensibility to drought, re-planted every season)

Costant F_q,

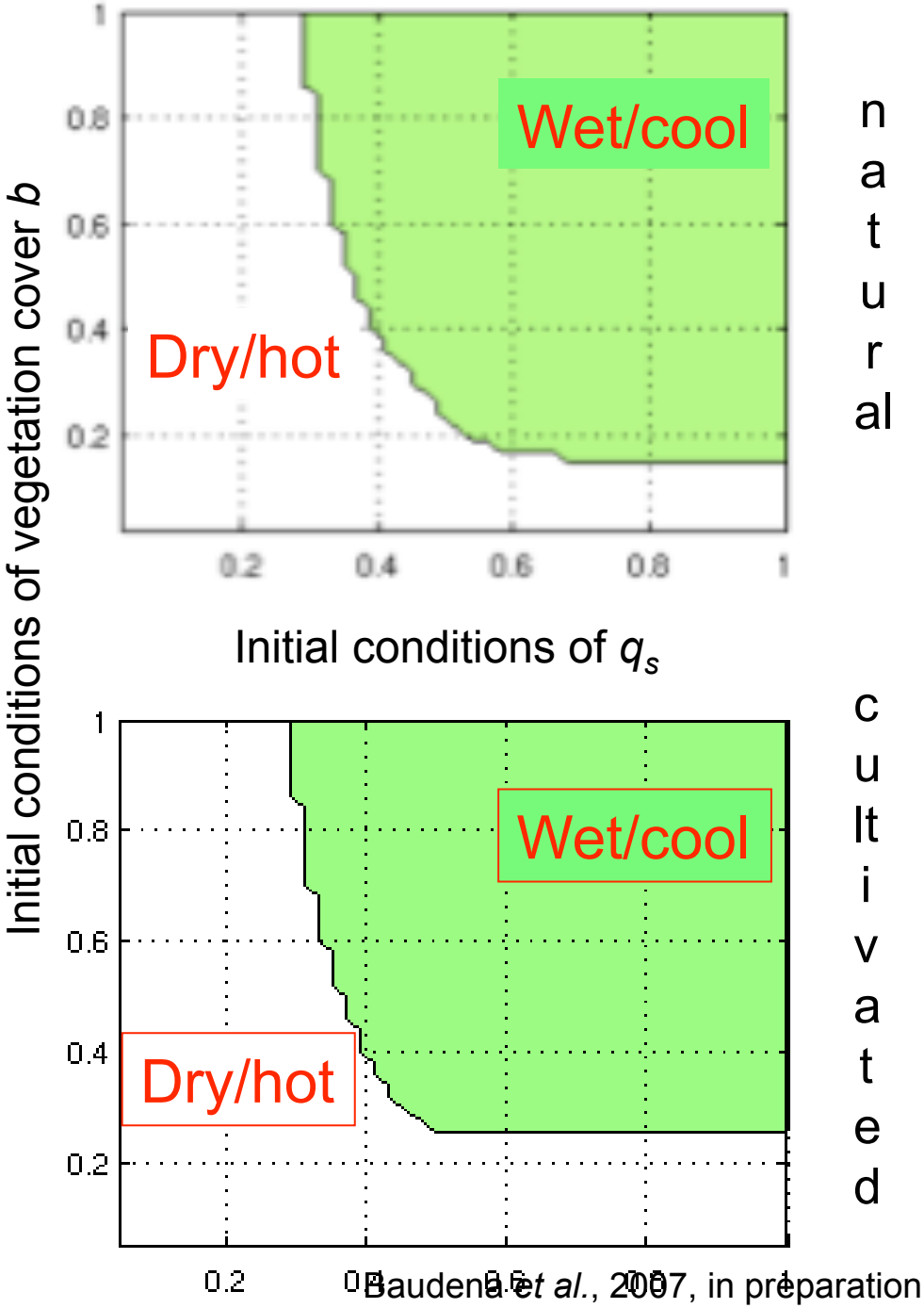

Baudena *et al.*, 2007, in preparation

Stochastic F_q, “natural” vegetation

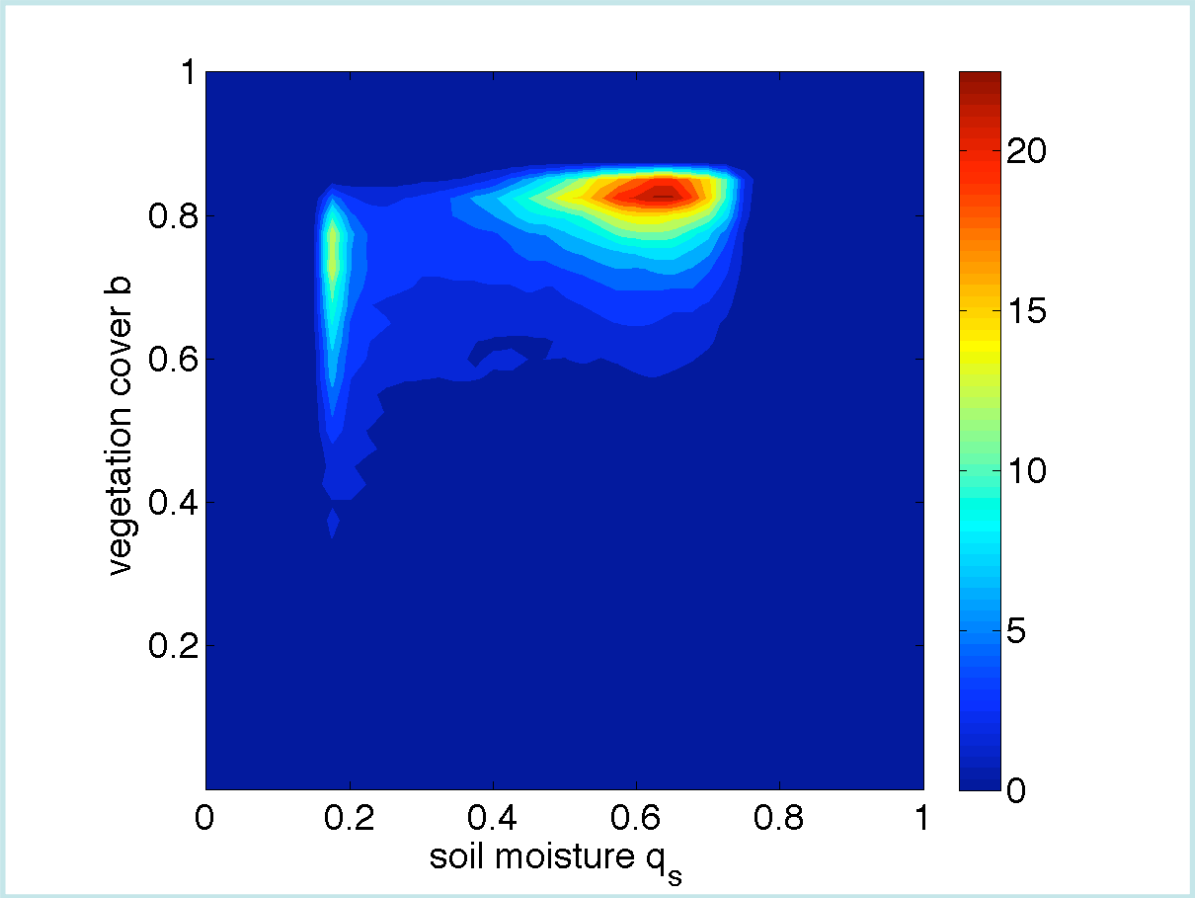

Baudena *et al.*, 2008, WRR.

Stochastic F_q, “cultivated” vegetation

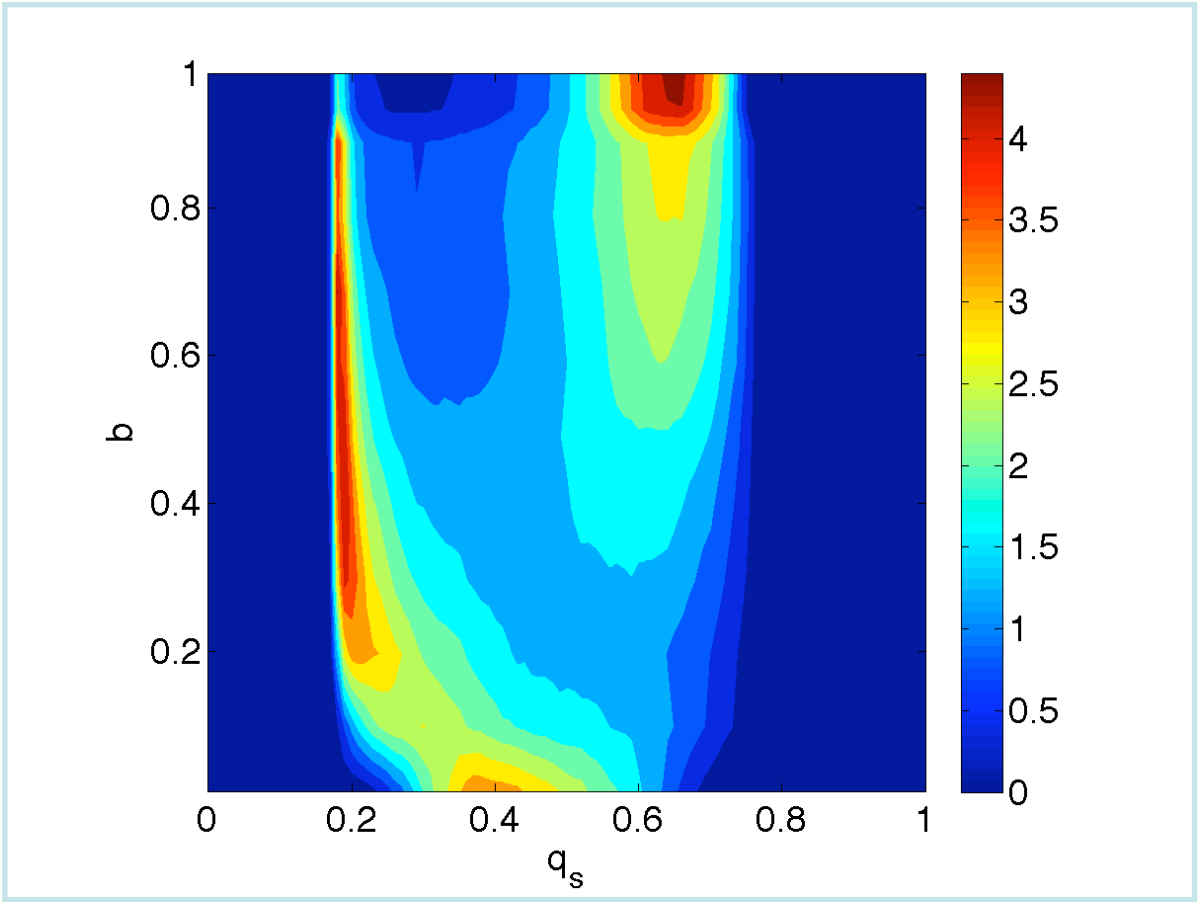

Baudena *et al.*, 2008, WRR.

3. Other mechanisms of soil moisture bimodality

D’Odorico and Porporato (PNAS 2006)
Porporato and D’Odorico, *Phys. Rev. Lett. 2004*

$$nZ\frac{\partial s}{\partial t} = I(s,t) - L(s)$$

The dependence of the probability of precipitation on the soil moisture is prescribed

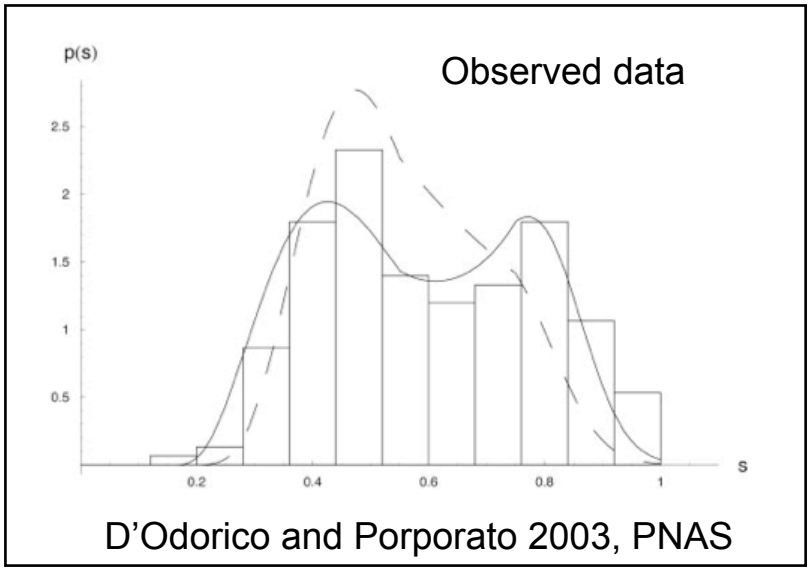

D’Odorico and Porporato 2003, PNAS

Daly et al (GRL 2009)

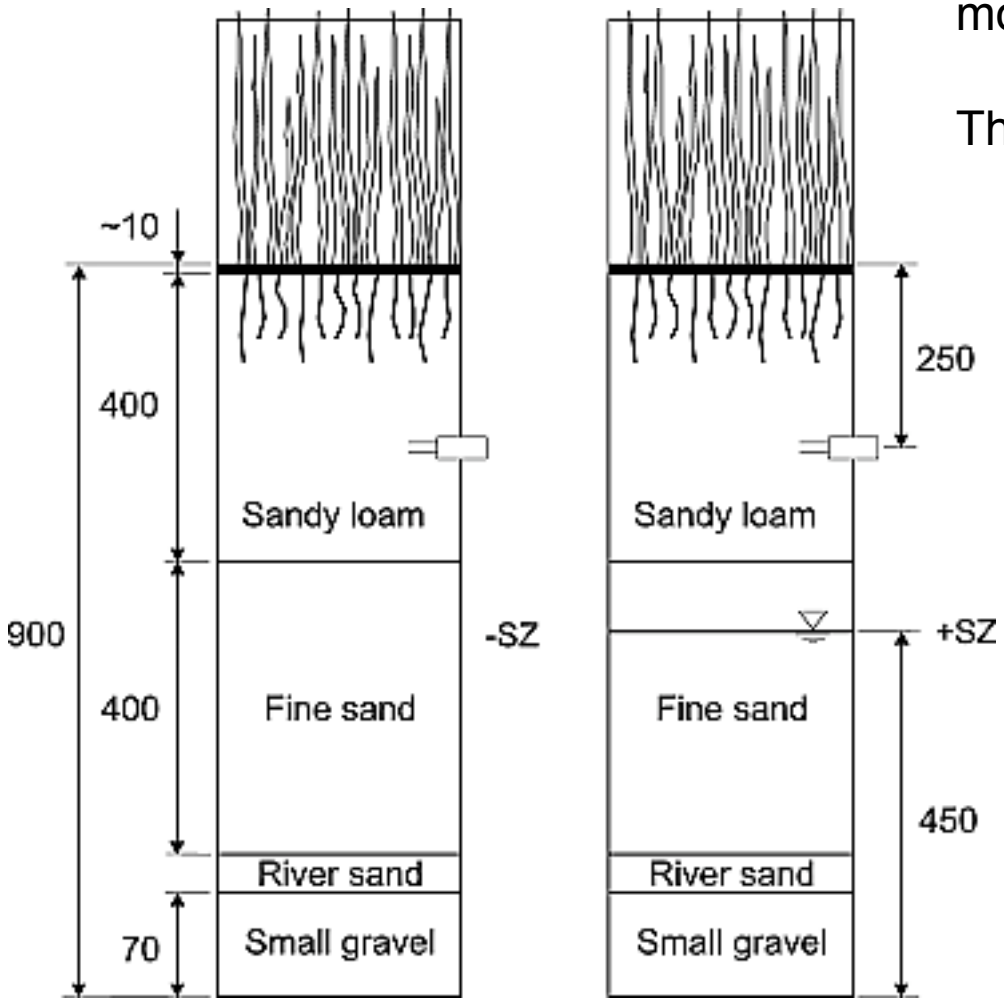

Capillary rise of water form a deep saturated layer can offset the loss of water at high moisture values.

The loss function $L(s)$ looks like this:

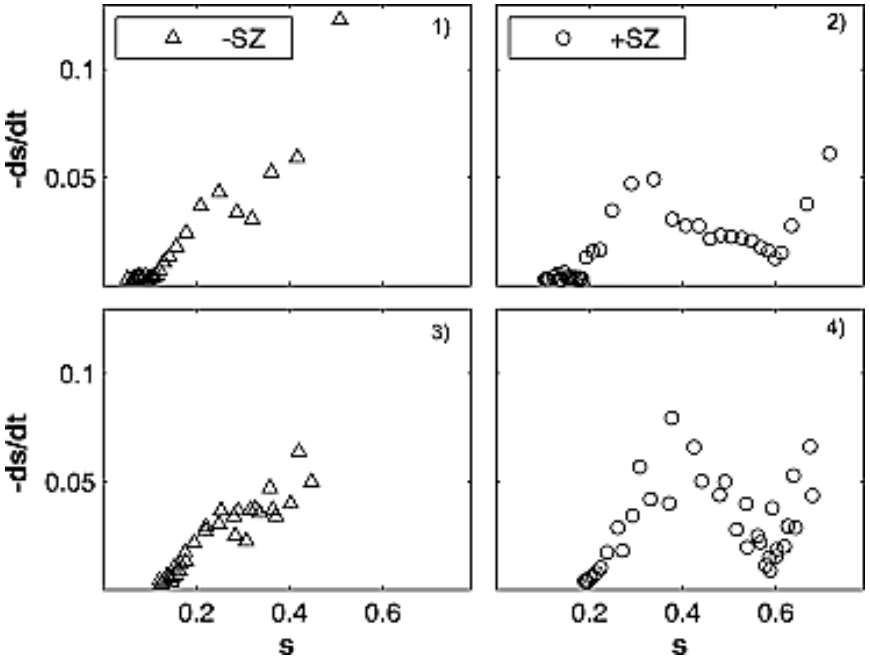

Teuling et al (GRL 2005): there is no evidence of feedback: “Here we show that seasonality in the meteorological conditions in combination with the nonlinearity of the soil moisture response alone can induce this bimodality. »

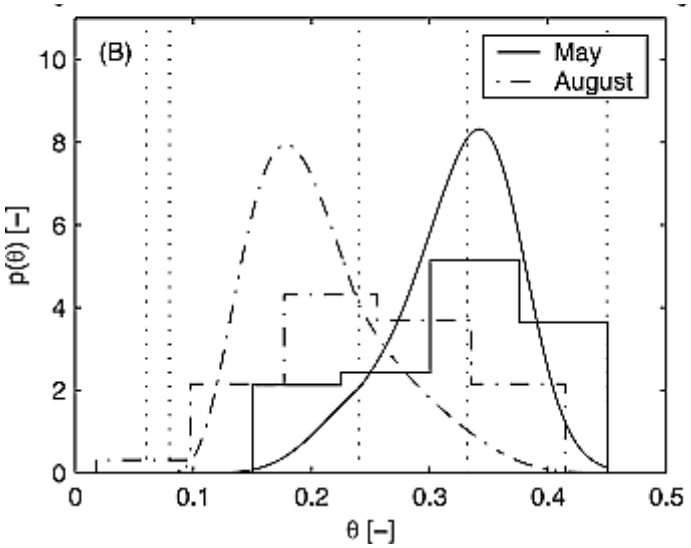

Lee and Hornberger (GRL 2006): There is bimodality also at shorter time-span:

August:

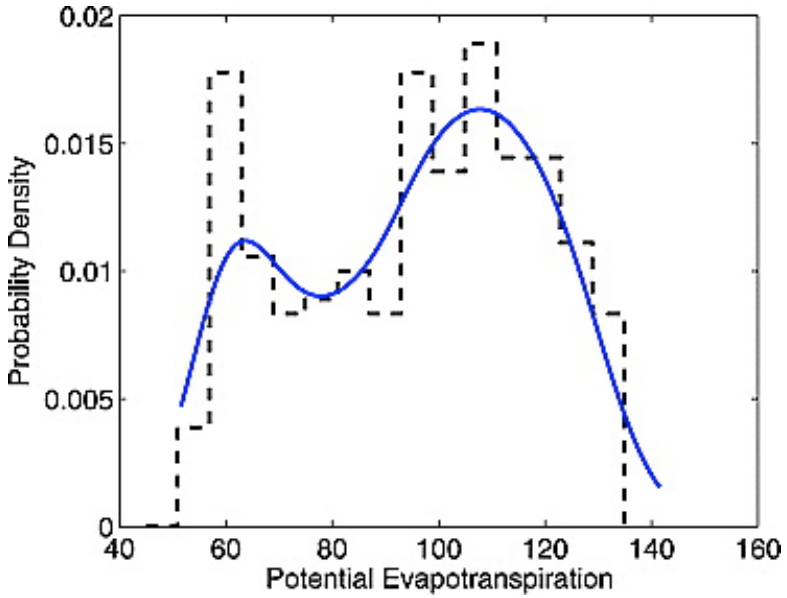

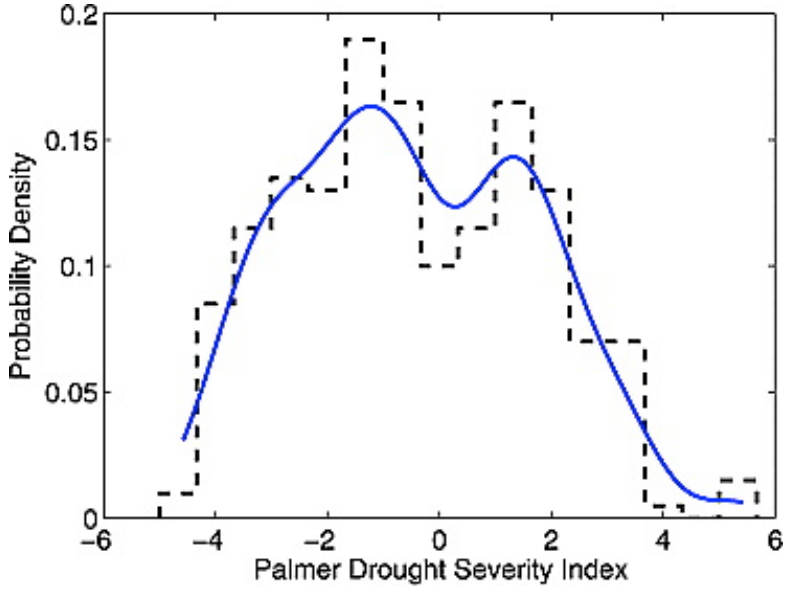

Symbol	Meaning	Value	
F_{sw}	Solar radiation at surface	380	$W\ m^{-2}$
L_e	Specific latent heat of Evaporation	$2.501\ 10^6$	$J\ Kg^{-1}$
R	Ideal gas constant	287	$J\ kg\ K^{-1}$
c_{pa}	Air specific heat	1000	$J\ kg^{-1}\ K^{-1}$
c_{ps}	Soil specific heat	1000	$J\ kg^{-1}\ K^{-1}$
h_a	Thickness of the atmospheric boundary layer	1000	m
h_s	Depth of the soil active layer	0.5	m
w_0	Soil water holding capacity	1500	$kg\ m^{-3}$
ϵ_b	Blackbody absorptivity of the PBL	0.3	
ϵ_s	Blackbody emissivity of the Earth	0.8	
ρ	Air density	1	$Kg\ m^{-3}$
ρ_s	Soil density	1800	$Kg\ m^{-3}$

Symbol	Meaning	Value	
C_D	Bulk aerodynamic drag coefficient	0.008	
E_{Max}	Maximum Potential Evapotranspiration	$1.5\ 10^{-4}$	$Kg\ m^{-2}\ s^{-1}$
E_w	Evapotranspiration at wilting point	$5\ 10^{-6}$	$Kg\ m^{-2}\ s^{-1}$
q_w	Wilting point	0.18	
q_h	Hygroscopic point	0.14	
q^*	Maximum plant efficiency point	0.46	
q_{fc}	Field capacity	0.56	
K_s	Saturated hydraulic condutiviy	0.03	$m\ d^{-1}$
β	parameter of water retention	14.	

ears	**1950**	**1952**	**1959**	**1964**	**1976**	**1983**	**1992**	**1994**	**1995**	**2003**
ummer T’	1.33	1.14	1.29	0.52	0.57	0.75	0.66	1.04	0.65	2.44
ummer P’	9	-23	-20	-18	-55	-54	+16	-29	-30	-58
ummer F’	+1.1	-1.0	-4.3	-2.1	-7.2	-8.1	+0.5	-4.9	-3.7	-9.2
4 d HW Start	02/06	28/06	05/07	14/07	22/06	06/07	29/07	24/07	08/07	01/08
4-day HW T’	2.91	3.77	2.79	2.65	4.07	2.83	1.93	3.38	2.44	4.19

Northward propagation of drought
(Vautard et al 2007, *GRL*)

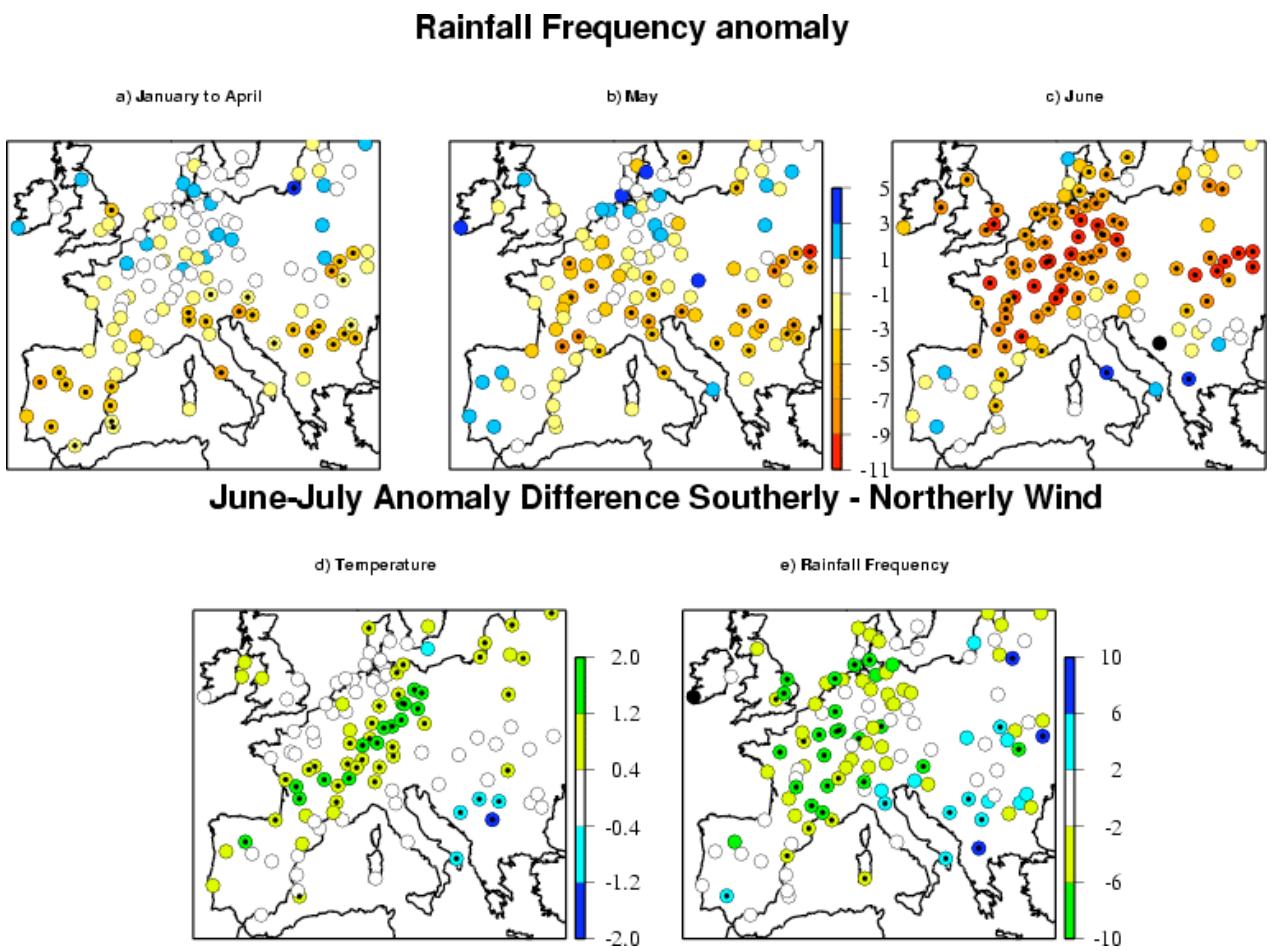

Figure: a) Average rainfall frequency anomaly (% of days) (January–April) for the 10 years containing the hottest summers listed in Table 1 of the Auxiliary Material. The color scale is as in Figure 1b. The figures that would obtain for the winter only (January-march, not shown) or from January to May are rather similar to this one; b) Same as a) for averages of the month of May only; c) Same as a) for June; d) Difference between the early summer (June and July) maximal hot-summer temperature anomalies when southerly wind occurs at the station and that obtained for northerly wind. At each station, days are classified into 2 classes according to the sign of the mean daily surface meridional wind field. The 58-year average maximal temperature is calculated and subtracted from the hot-summer average to obtain mean anomalies. Then the difference between "southerly" and "northerly" mean anomalies is shown in panel d). The figure shows that temperature anomalies, in the 10 hottest summers, are higher in southerly wind conditions than in northerly wind conditions. e) As in d) for rainfall frequency (% of days). Stations where the differences are significant at the 90% level are marked with a black bullet.

A predictor in the mediterranean region?

Spring precipitation at different band of latitude and summer temperature

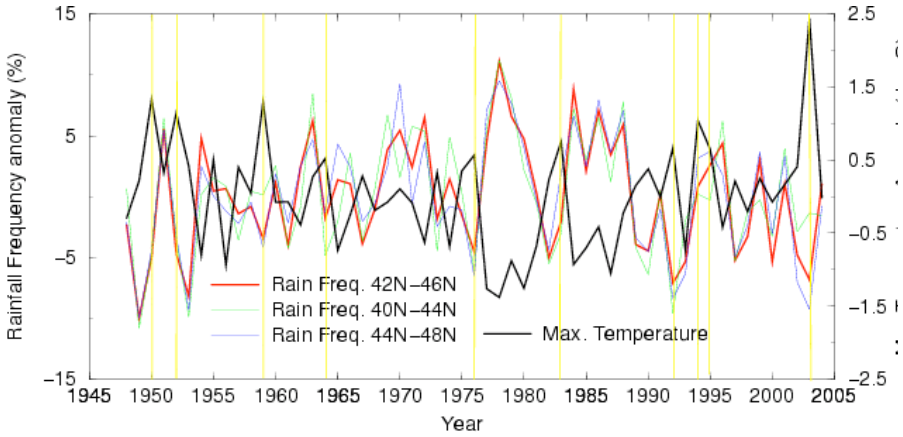

Figure 3: Detrended summertime (JJA) daily maximum temperature anomalies, averaged over European stations, as a function of year (in black), together with the detrended anomaly of precipitation frequency averaged in the 42°N-46°N latitude band during preceding winter and early spring (January to May), in red. Temperature anomalies are in °C while precipitation frequencies anomalies are in %. In order to assess the sensitivity to the chosen latitude band for precipitation frequency, 2° northward and southward shifts are applied and results are also represented. Yellow bars indicate the years selected in the hottest 10 summer years.

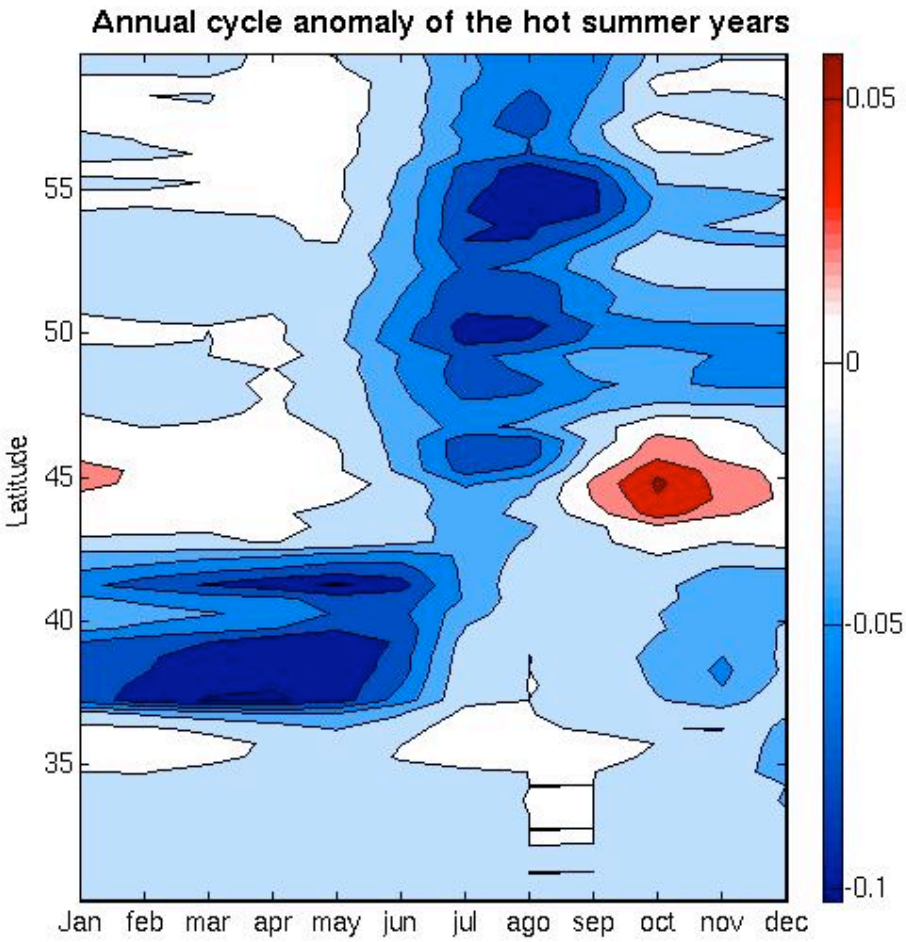

Data from weather stations + a water budget model. Wilmott and Matsuura 2001.

RESEARCH HIGHLIGHTS

EXTREME EVENTS

Rainfall rules

Geophys. Res. Lett. **34**, L07711 (2007)

Checking Mediterranean rain gauges in winter may provide clues for predicting Europe's next deadly heat wave. Robert Vautard of France's Institut Pierre-Simon Laplace and colleagues have now discovered that a deficit of winter rainfall in southern Europe is a good indicator of high summertime temperatures and drought farther north.

Using meteorological data from over 100 sites in Europe, Vautard's team analysed the ten hottest European summers between 1948 and 2005, including 2003 when some 35,000 people died. All were preceded by southern European winters of below average rainfall. The water reservoir in Mediterranean soils plays a crucial role in maintaining this link, the researchers say.

During dry southern winters, soils release little moisture to the atmosphere. As a result, southerly winds blow warm dry air northward, reducing cloud cover and warming the air. Northern soils also dry faster, causing further warming from below. Scientists expect southern Europe to become increasingly dry, triggering more frequent heat waves and drought, as a result of climate change. Authorities can better prepare for extreme summer heat by studying rainfall patterns in the Mediterranean each winter.

Harvey Leifert

nature

ACCUEIL

LE FIGARO.fr

MULTIMÉDIA
Faut-il craquer pour la PlayStation 3 ?

ACTUALITÉ | ÉCO-BOURSE | SPORTS | CULTURE LOISIRS | madame | PATRIMOINE | EMPL

Actualité | Sciences & Médecine

Les canicules naissent après des hivers secs en Méditerranée

YVES MISEREY. Publié le 29 mars 2007

Actualisé le 29 mars 2007 : 08h29

COLONNES T– T+

Les étés torrides sur l'Europe de l'Ouest sont toujours précédés par des hivers secs dans le nord de la Méditerranée occidentale. Une situation rencontrée cet hiver, et qui pourrait annoncer une canicule.

QU'EST-CE qui déclenche les canicules en France et plus généralement en Europe de l'Ouest ? Quelles sont les données climatiques qui peuvent permettre de les prévoir alors même que le réchauffement laisse présager qu'elles risquent de devenir plus fréquentes ? La canicule de 2003 qui a fait 70 000 morts en Europe de l'Ouest selon le bilan présenté à l'OMS la semaine dernière, a évidemment fait émerger de nouvelles questions. Robert Vautard, directeur du LSCE (laboratoire des sciences du climat de Saclay/CEA, CNRS) et Pascal Yiou, lui aussi du LSCE, se sont posé la question. Après de longues discussions sur le lien entre canicule et sécheresse lors de fréquentes rencontres sur un marché, ils ont décidé de s'y intéresser de près. Et ils publient leurs résultats dans le prochain numéro des *Geophysical Research Letters*.

Leur étude montre, et c'est nouveau, que les canicules en France sont toujours associées à des hivers secs dans une large bande, allant de l'Espagne au nord de l'Italie en passant par les Pyrénées et le Midi de la France. « *C'est la naissance du signal* », explique Pascal Yiou. C'est nécessaire mais toutefois pas suffisant. Pour que la canicule s'installe véritablement, en effet, il faut en plus que la circulation atmosphérique soit bloquée durant l'été sur l'ouest de l'Europe. Or le blocage, lié à la présence d'un anticyclone, est très aléatoire et donc imprévisible. « *En 2005, j'avais parié que l'été allait être caniculaire car l'hiver avait été sec en Espagne et dans le sud de la France. Juin a été très chaud comme prévu mais un flux nord et ouest s'est installé en juillet et il n'y a pas eu de canicule* », raconte le chercheur. Selon lui, la probabilité est de 70 à 90 %.

ZOOM

L'est de l'Espagne touché par la sécheresse. Bustamante/AP.

Les autres titres

- La circoncision, une arme contre le sida
- Pour Bruxelles, tous les poissons doivent rester à bord
- Pourquoi faut-il bénir la petite boîte de Richard Petri ?
- Jakarta et l'OMS partageront leurs échantillons de virus H5N1
- Chirac fait le bilan de cinq années de plan cancer

MM5 Integration details **(**credit: Matteo Zampieri, LMD)

Simulations domain: most of Europe (excluding the Northern part of the Scandinavian peninsula) and a large part of the Atlantic Ocean.

Forced by the ECMWF (ERA40) or NCAR-NCEP reanalyses with a 6-hour rate.
Resolution: 36 km at the centre of the domain. 85x125 grid points and 23 vertical levels.
MM5 3.7.3 model version
Reisner microphysics,
Kain-Fritsch convection scheme,
MRF PBL scheme
CCM2 radiation scheme.
NOAH land-surface 4-layer scheme.

twin simulation, starting on 1 June, for all the 10 hottest summers, differing only by their initial soil moisture south of 46N:

1) 'wet' simulation. Initial volumetric soil moisture content of 30% .
2) 'dry' simulation Initial volumetric soil moisture content of 15%.

North of 46N initial soil moisture content is taken from the ERA40 ECMWF reanalysis data, when possible, or the NCAR-NCEP reanalysis data.

European heatwaves are preceded by drought in the mediterranean region: analysis of the physical processes involved by regional modelling.

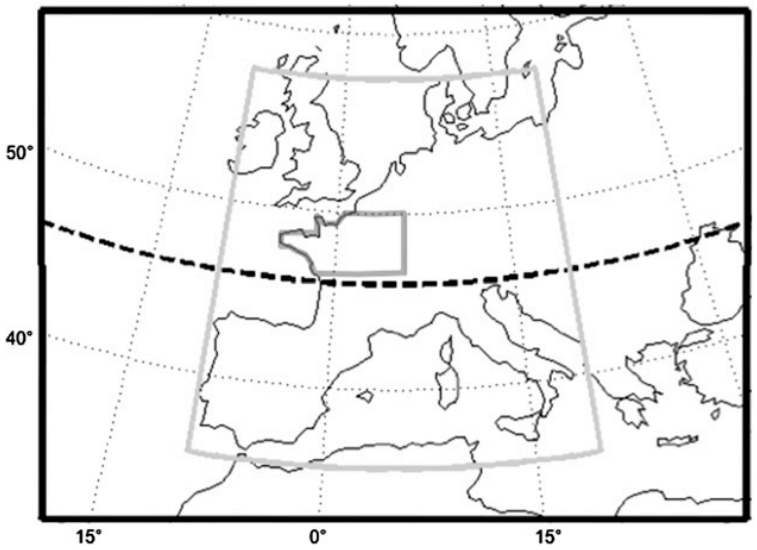

twin simulation of MM5, starting on 1 June, for all the 10 hottest summers on record, differing only by their initial soil moisture south of 46N:

1) 'wet' simulation. Initial volumetric soil moisture content of 30% .
2) 'dry' simulation Initial volumetric soil moisture content of 15%.

Propagation of temperature Anomaly (dry-wet runs):

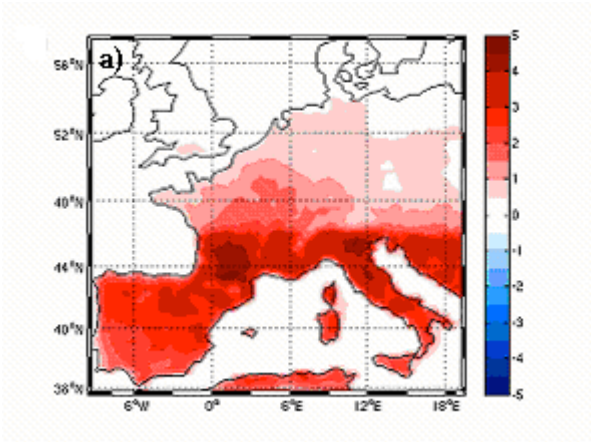

Evolution of incomig solar radiation (left, red line) and of the bowen ratio (right, red line), dry-wet run.

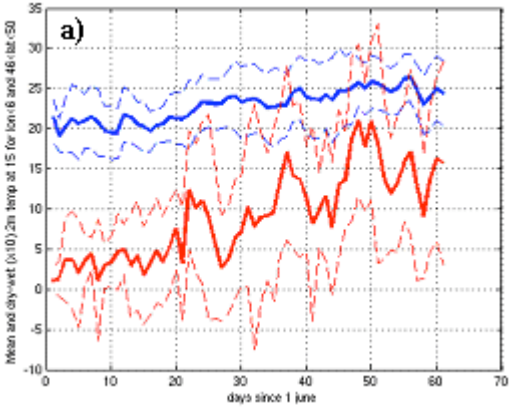

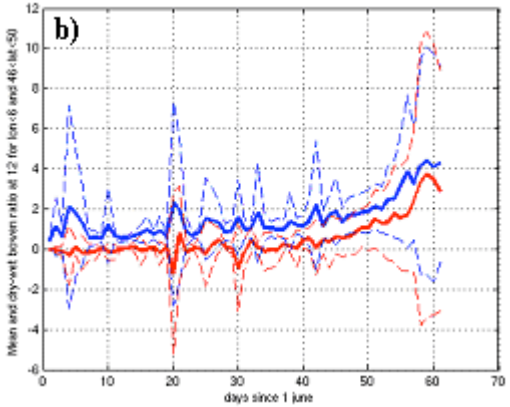

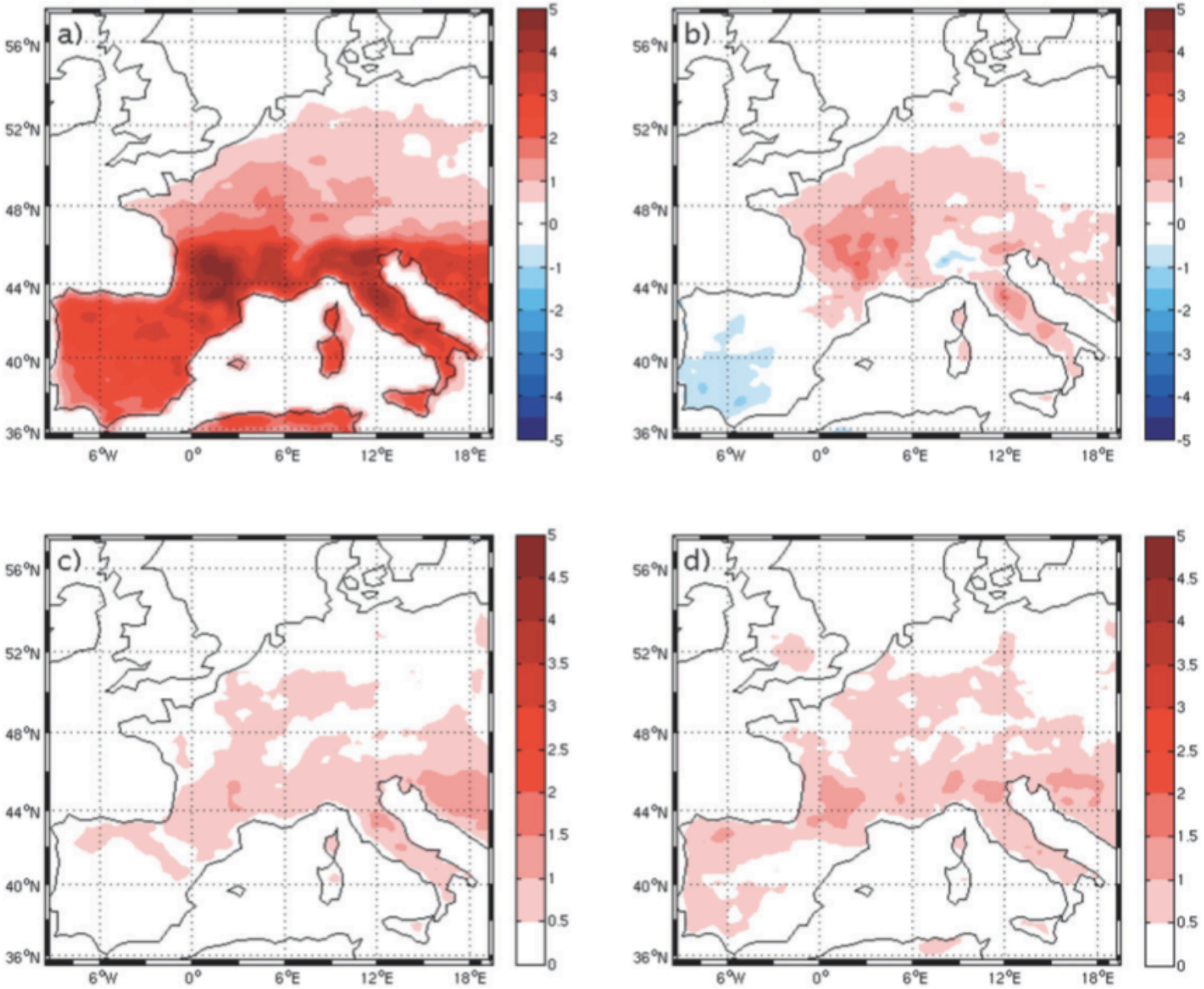

FIG. 4. Results from the sensitivity (DRY and WET) simulations averaged over the 10 hottest summers of the last 50 years: (a) difference (DRY minus WET) of 1500 UTC 2-m temperature averaged over the month of July; (b) difference of July minus June of the DRY minus WET field at 1500 UTC for 2-m temperature (an increment of the DRY − WET differences). (c),(d) Temperature (interannual) standard deviation across the 10 individual summers of the variables plotted in (a) and (b), respectively.

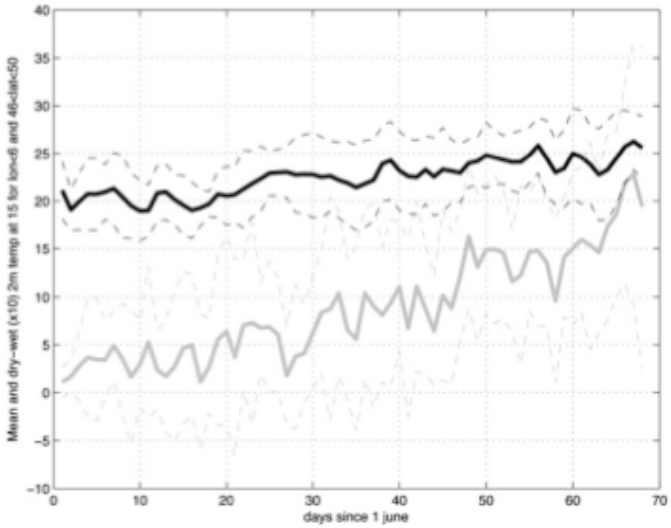

FIG. 5. Average time evolution over the 10 hottest summers of 2-m temperature at 1500 UTC averaged between 46.5° and 50°N and for longitude between the Atlantic coast and 6°E. The mean of DRY and WET results is in black, and the difference is in grey. The dashed lines represent the corresponding 1 std dev bands. The difference is multiplied by 10.

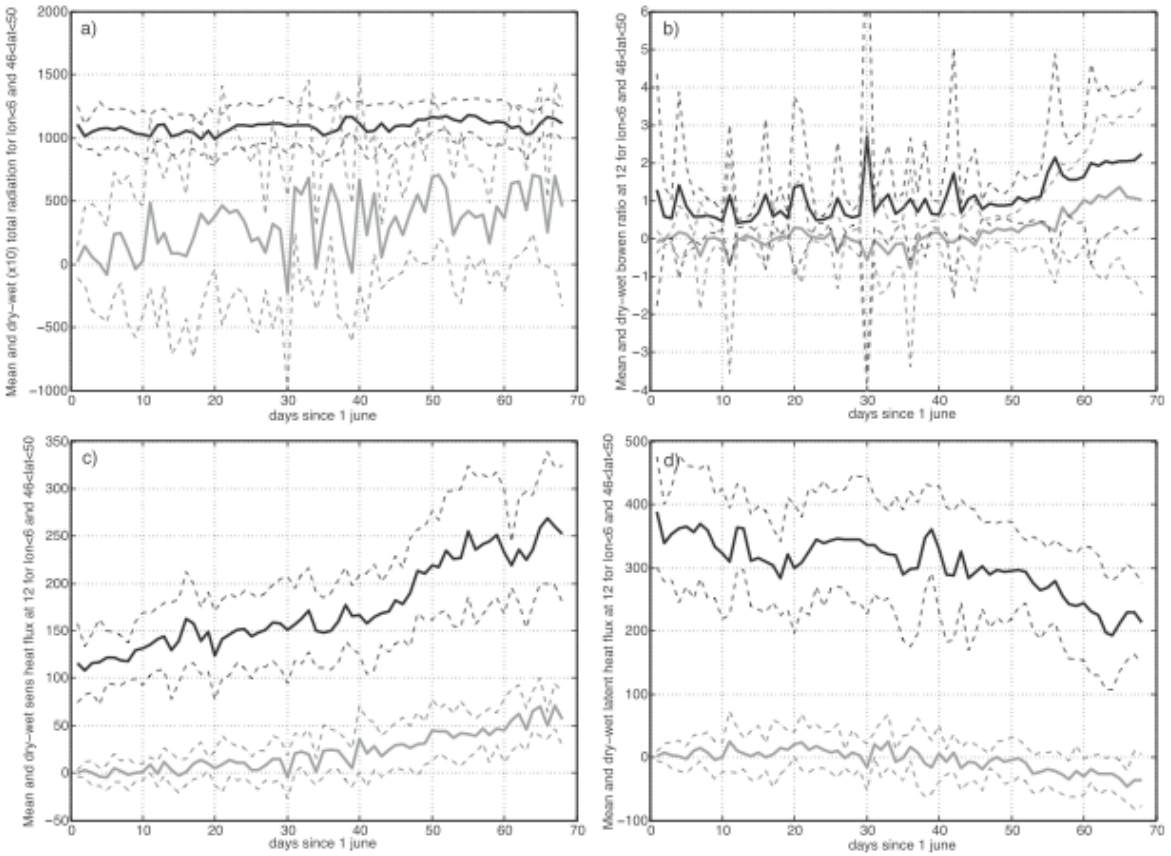

FIG. 11. Same as Fig. 5, but for (a) total net incoming radiation at the surface, (b) the Bowen ratio, defined as the ratio of sensible to latent heat fluxes, (c) sensible heat flux, and (d) latent heat flux. Differences of incoming radiation are multiplied by 10 for readability.

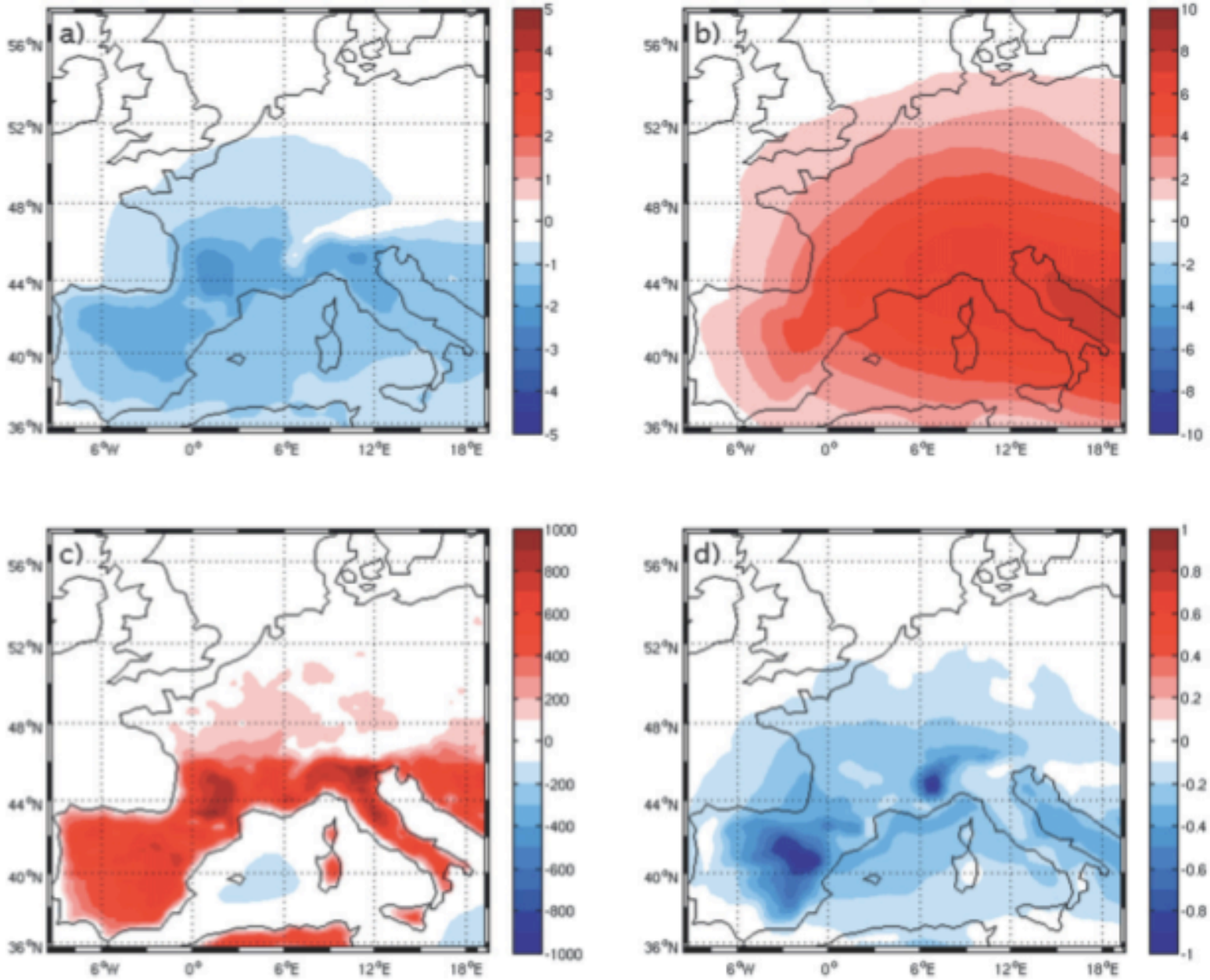

FIG. 12. DRY minus WET mean July anomaly of (a) mean sea level pressure (mb), (b) geopotential at 500 mb (m), (c) boundary layer height at 1500 UTC (m), and (d) lapse-rate between 700 and 500 mb (K km^{-1}).

Drier soils favor :

1) higher sensible heat fluxes and subsequent local warming

2) drier air with less and less extended clouds, leading to enhanced solar radiation.

3) lesser convection, leading to increased PBL height and to the development of upper-air anticyclonic circulation conditions.

A simple model of the interaction of the land surface and the atmospheric planetary boundary layer

1. Box model 1 - the soil moisture - precipitation feedback
2. Box model 2 - the effect of vegetation dynamics

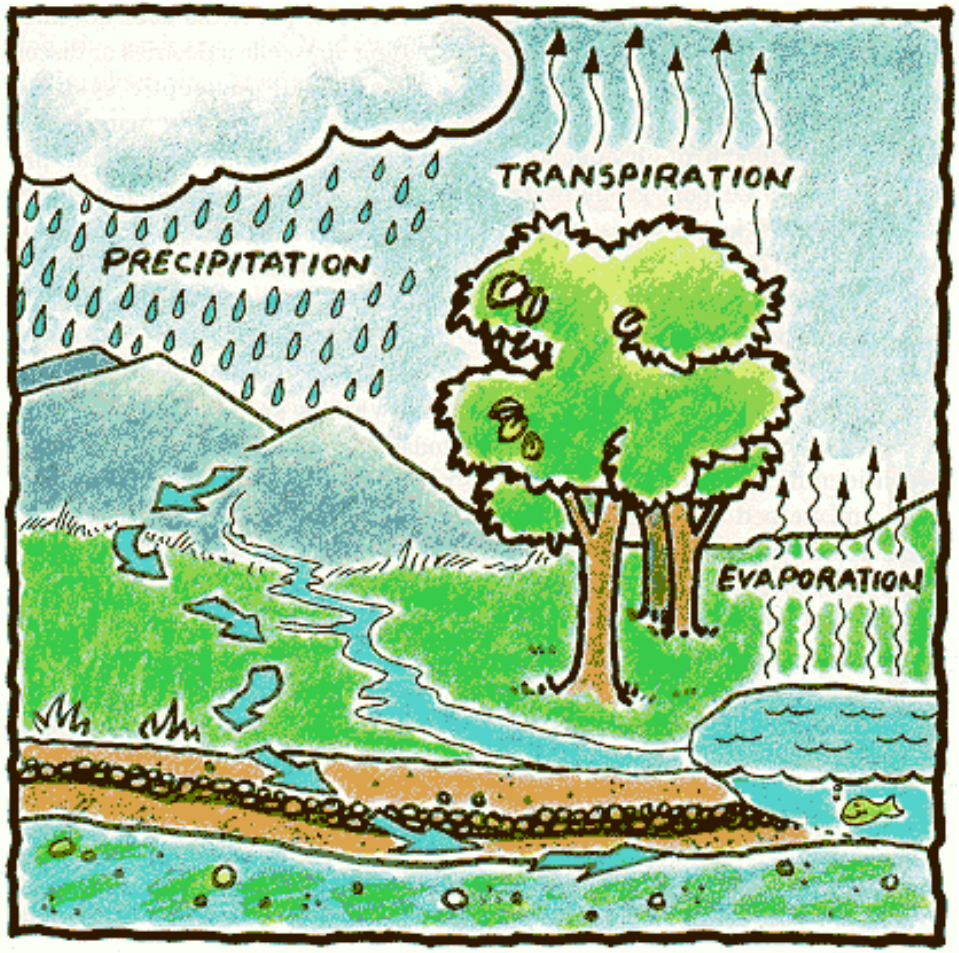

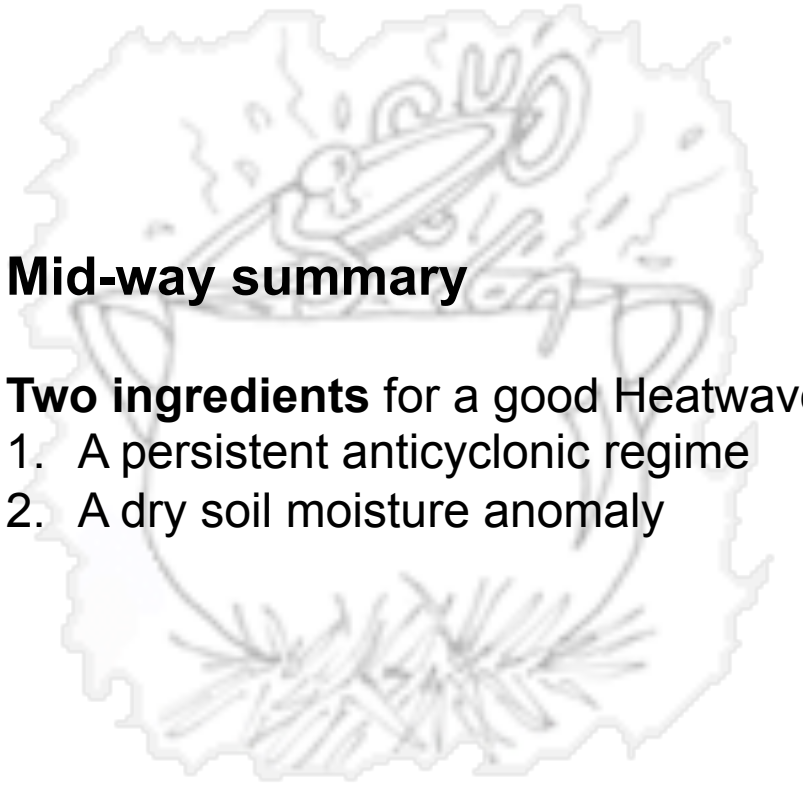

Mid-way summary

Two ingredients for a good Heatwave:

1. A persistent anticyclonic regime
2. A dry soil moisture anomaly